

1 A 6,000-year record of environmental change from the eastern Pacific margin of  
2 central Mexico

3

4 Sarah J. Davies<sup>a</sup>, Sarah E. Metcalfe<sup>b</sup>, Benjamin J Aston<sup>a\*</sup>, A. Roger Byrne<sup>c†</sup>, Marie R.  
5 Champagne<sup>d</sup>, Matthew D. Jones<sup>b</sup>, Melanie J. Leng<sup>e,f</sup>, Anders Noren<sup>g</sup>

6

7 <sup>a</sup> Department of Geography and Earth Sciences, Aberystwyth University, Penglais,  
8 Aberystwyth, SY23 3DB, UK. Corresponding Author (sjd@aber.ac.uk).

9 <sup>b</sup> School of Geography, University of Nottingham, University Park, Nottingham, NG7  
10 2RD, UK.

11 <sup>c</sup> Department of Geography, University of California at Berkeley, 505 McCone Hall  
12 #4740, Berkeley, CA 94720-4740, USA.

13 <sup>d</sup> Quaternary Paleoenvironmental Research Laboratory, Geology, Minerals, Energy  
14 and Geophysics, U.S. Geological Survey, 345 Middlefield Road, MS 975, Menlo Park,  
15 CA 94025, USA.

16 <sup>e</sup> NERC Isotope Geosciences Facilities, British Geological Survey, Keyworth,  
17 Nottingham, NG12 5GG, UK.

18 <sup>f</sup> Centre for Environmental Geochemistry, School of Biosciences, Sutton Bonington  
19 Campus, University of Nottingham, Loughborough, LE12 5RD, UK.

20 <sup>g</sup> Continental Scientific Drilling Coordination Office and LacCore Facility, Department  
21 of Earth Sciences, University of Minnesota, 500 Pillsbury Drive  
22 SE, Minneapolis, Minnesota 55455, USA.

23

24 \* Current address: Yorkshire Water, Environment Assessment Team, Western House,  
25 Western Way, Bradford, BD6 2SZ

26

27 † Deceased

28

29 Declarations of Interest: None

30

31 © 2018. This manuscript version is made available under the CC-BY-NC-ND 4.0

32 license <http://creativecommons.org/licenses/by-nc-nd/4.0/>



34

35 Abstract

36

37 The transition from the mid- to late-Holocene in MesoAmerica saw increasing  
38 complexity in spatial patterns of change. Records from the western part of the  
39 region are sparse, with lacustrine sequences affected by long term anthropogenic  
40 disturbance or lacking chronological resolution. Here, we present a continuous  
41 palaeoecological and geochemical record from Laguna de Juanacatlán, a remote lake  
42 in the mountains of the western TMVB. Diatom assemblages, XRF scanning data and  
43 bulk organic geochemistry from a well-dated, 7.25-m laminated sequence were  
44 combined with summary pollen data from a 9-m partially laminated core to provide  
45 a continuous record of catchment and lake ecosystem changes over the last c. 6,000  
46 years. Relatively humid conditions prevailed prior to c. 5.1 cal ka, which supported  
47 dense oak-pine forest cover around a deep, stratified lake. A trend towards drier  
48 conditions began c. 5.1 cal ka, intensifying after 4.0 cal ka, consistent with weakening  
49 of the North American Monsoon. Between 3.0 and 1.2 cal ka, lower lake levels and  
50 variable catchment run-off are consistent with increasing ENSO influence observed  
51 in the Late Holocene in the neotropics. From 1.2 to 0.9 cal ka, a marked change to  
52 catchment stability and more intense stratification reflected drier conditions and / or  
53 reduced rainfall variability and possibly warmer temperatures. After 0.9 cal ka,  
54 conditions were wetter, with an increase in catchment disturbance associated with  
55 the combined effects of climate and human activity. In recent decades, the lake  
56 ecosystem has changed markedly, possibly in response to recent climate change as  
57 well as local catchment dynamics.

58

59 Keywords: Holocene; Palaeolimnology; North America; diatoms; geochemistry;  
60 pollen.

61

62 1. Introduction

63

64 The broad pattern of climatic change across Mexico over the Holocene has become  
65 better understood over the last 20 years (c.f. Metcalfe et al., 2000 and Metcalfe et

66 al., 2015), but the spatial distribution, sampling resolution and chronological control  
67 of paleoclimate records from the region are highly variable. Generally wetter  
68 conditions in the early to mid-Holocene were driven by insolation forcing, and are  
69 associated with northward movement of the intertropical convergence zone (ITCZ)  
70 and strengthening the North American Monsoon (NAM). This was followed by a  
71 change around 4 cal ka, when the role of insolation declined. The ITCZ moved  
72 southward and the NAM weakened, leading to drier conditions over much of  
73 Mexico. A more complex set of climate forcings then seem to have become more  
74 evident, especially those associated with the tropical and sub-tropical Pacific, such as  
75 the El Niño Southern Oscillation (ENSO) and the Pacific Decadal Oscillation (PDO).  
76 Differences between southern and northern, and perhaps eastern and western  
77 Mexico, became more apparent. Some of this variability seems to be explained by  
78 spatially different responses to forcings such as the Atlantic Multi-Decadal Oscillation  
79 (AMO), the PDO and ENSO. The highlands of central Mexico, the Trans-Mexican  
80 Volcanic Belt (TMVB) (at about 20°N), appear to lie in the transition zone in terms of  
81 some of these responses (Stahle et al., 2012).

82

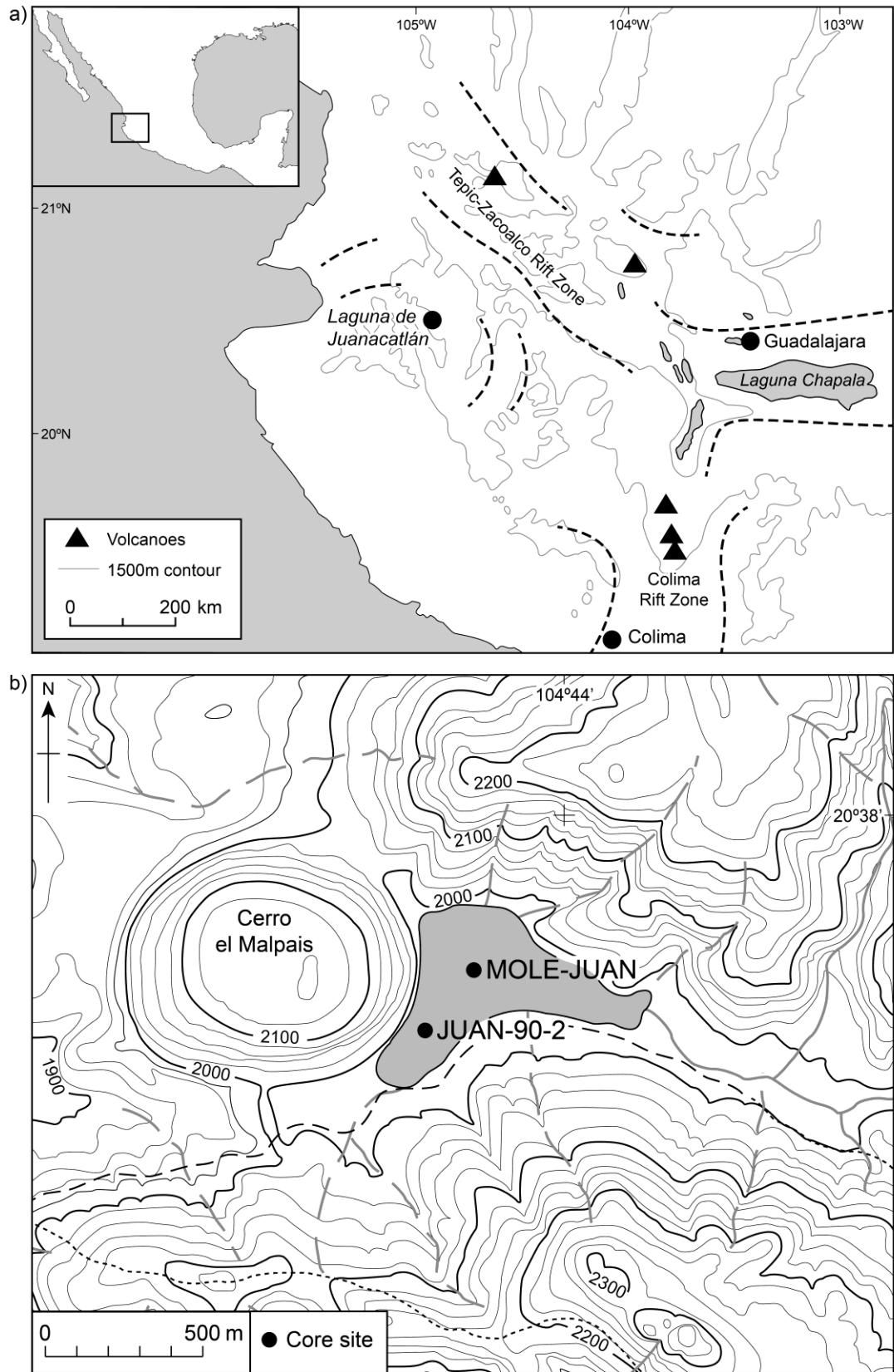
83 The many lake basins of the TMVB have long been a focus for palaeoclimate studies,  
84 particularly in and around the Basin of Mexico and in the states immediately west  
85 (Estado de Mexico, Michoacán). However, the number of continuous, high-  
86 resolution Holocene records from this part of Mexico remains small as  
87 sedimentation rates in basins are often quite low or discontinuous due to  
88 volcanic/tectonic activity, periodic desiccation and deliberate drainage (Caballero et  
89 al., 1999; Vázquez-Castro et al., 2008; Ortega et al., 2010). The situation is further  
90 complicated by the strong imprint of human activity on many Holocene records from  
91 the area, with *Zea mays* (domesticated maize) appearing in pollen records from  
92 around 4 ka (Watts and Bradbury, 1982; Lozano-García et al., 2013). Large increases  
93 in sedimentation rates also occurred, coincident with the onset of sedentary  
94 agriculture (O'Hara et al., 1993; Metcalfe et al., 1994; Vázquez-Castro et al., 2010). In  
95 some cases, it has been difficult to develop reliable radiocarbon chronologies  
96 because of inwash of old carbon from catchments (Metcalfe et al., 1994). Only sites  
97 at very high elevations, close to the modern timberline, seem to have been immune

98 from anthropogenic influence (Lozano-García and Vázquez-Selem, 2005).  
99 Development of continuous, high-resolution palaeoclimate records from maar lakes  
100 across the TMVB, which often preserve laminated sediments, is now being realised  
101 (Sosa-Nájera et al., 2010; Bhattacharya et al., 2015; Rodríguez-Ramírez et al., 2015;  
102 Park et al., 2017) and new, high-resolution sequences have been produced for the  
103 southern Mexican highlands (Goman et al., 2018), though these show clear evidence  
104 of long-term human impact.

105

106 Here we present a record from remote highland lake Laguna de Juanacatlán, on the  
107 western fringe of the TMVB, which spans the mid-late Holocene. Laguna de  
108 Juanacatlán (Fig. 1) lies close to the area that is often considered to be the 'core' of  
109 the North American Monsoon (Douglas et al., 1993; Ropelewski et al., 2005). The site  
110 was first investigated in 1990, and its often-laminated sediments demonstrated the  
111 potential for development of a high-resolution palaeoclimatic record (Byrne et al.,  
112 1996). Our initial research at the site used diatoms from the last few hundred years,  
113 in a suite of short cores, and highlighted rapid, recent changes in the aquatic  
114 ecosystem (Davies et al., 2005). Collection of longer cores (see below) and  
115 application of micro-XRF scanning of the finely laminated sediment sequence  
116 enabled development of an annually resolved rainfall reconstruction for the last  
117 6,000 years, based on the titanium record (Metcalf et al., 2010; Jones et al., 2015).  
118 This long-core sequence provides a complete, high-resolution sequence from this  
119 part of Mexico for the last 6 cal ka. In this paper, we synthesise the geochemical (XRF  
120 scanning, bulk organic geochemistry) and palaeoecological (diatoms, pollen)  
121 evidence from Juanacatlán to explore links between Holocene climate variability,  
122 including the NAM, lake dynamics and vegetation change, providing insights into the  
123 complex drivers of change from a uniquely well-dated sequence.

124



125

126 **Figure 1: a) Regional setting of Laguna de Juanacatlán and b) the local catchment,**

127 **illustrating core locations.**

128

129 2. Regional Setting

130

131 Laguna de Juanacatlán (20°37'N, 104°44'W) is a lava-dammed lake situated in a  
132 remote location in the Sierra de Mascota (Fig. 1) at ~2000 m a.s.l, approximately 52  
133 km east of the Pacific Coast at Puerto Vallarta. It lies within the Mascota Volcanic  
134 Field (MVF), in the Jalisco Block (Fig. 1a), which is bounded to the northwest by the  
135 Tepic-Zacoalco Rift Zone and to the east by the Colima Rift Zone (Carmichael et al.,  
136 1996). The MVF is characterised by an unusual diversity of volcanic rocks, dominated  
137 by potassic and hydrous types that range in composition from minettes to andesites.  
138 Potassium-argon dating of volcanic deposits in the MVF indicates an age range from  
139 c. 5 ka to 2.48 Ma (Carmichael et al., 1996; Ownby et al., 2008).

140

141 The lake surface area is approximately 0.5 km<sup>2</sup> within a 10 km<sup>2</sup> catchment, and the  
142 water body is surrounded by steep slopes that rise to a maximum of 2,300 m a.s.l.  
143 The closest meteorological station is at Mascota, 800 m lower and 12 km away from  
144 the lake. Average annual temperature at Mascota is 21.8°C and average annual  
145 precipitation is 1026 mm (IMTA, 1996). Lake water has a calcium-magnesium  
146 bicarbonate composition (Davies et al., 2002), with a pH range of 7.8-8.8 and  
147 electrical conductivity from 100 to 150 µS cm<sup>-1</sup>. Thermal stratification of the water  
148 column was evident on each field visit between 1998 and 2006, with seasonal  
149 variation in depth. In July 2005 (wet season) the thermocline was observed between  
150 3 and 6 m depth, whilst at the end of the following dry season (April 2006), the  
151 thermocline was between 6 and 8 m depth. Results of more recent sampling in  
152 October 2011 (Sigala et al., 2017) were consistent, with the onset of the thermocline  
153 observed at 7 m depth.

154

155 Pine (*Pinus*) or pine/oak (*Quercus*) forests are typical of west-central Mexico at  
156 elevations between 1200 and 3000 m (Ortega Rosas et al., 2008; Lozano García et al.,  
157 2013). In a study of modern vegetation just north of Juanacatlán, Guerrero-  
158 Hernandez et al. (2014) reported *Quercus obtusata*, *Q. scytophylla*, *Q. candicans*,  
159 *Pinus devoniana* and *P. lumholtzii* as dominant forest species. These authors also  
160 described *Abies* (fir) forest (mainly *A. flinckii*), but noted its rather restricted

161 distribution. The area shows a high level of endemism, with an estimated 35% of  
162 forest species being endemic to Mexico, nearly 5% endemic to the state of Jalisco  
163 and 4% endemic to the western highlands within the state (Guerrero-Hernandez et  
164 al., 2014). Within the Juanacatlán Basin, there is a concentration of oak on an  
165 apparently recent volcanic dome (Cerro el Malpais) at the west end of the lake (Fig.  
166 1b). Prior to recent development of the catchment for tourism, *Salix* (willow) was  
167 common along the lake shore and particularly in the southwest, where there is an  
168 extensive area of flatter land. Core JUAN-90-2 was taken close to this area (see  
169 below).

170

171 The regional archaeological context of western Mexico is characterised by shaft  
172 tomb cultures, represented at various sites in Michoacán, Nayarit and Jalisco, the  
173 earliest dating from around 1400 BCE. The Late Formative and Classic (300 BCE – 500  
174 / 600 CE) was a period of population growth and expansion and saw the  
175 development of ceremonial architecture represented by distinctive circular, stepped  
176 pyramids as found at Guachimontones (Beekman, 2010), c. 150 km from  
177 Juanacatlán. Little is known about the prehistory of the immediate surroundings of  
178 Laguna de Juanacatlán, but middle-Formative (c. 800 BCE) burial sites have been the  
179 subject of recent investigations in the Mascota Valley (Rhodes et al., 2016), where  
180 there are also numerous Pre-Hispanic petroglyphs (Mountjoy, 2012). Colonial silver  
181 and gold mining was established in the 17<sup>th</sup> century in the Sierra de Mascota, but it is  
182 unclear if there were operations within the catchment itself (Davies et al., 2005).

183 During the 1950s, a channel was dug at the southwest end of the lake to supply  
184 irrigation water to small farms in the adjacent valley. Until the late 1990s, catchment  
185 disturbance was very low in comparison with other central Mexican lake basins, and  
186 there was little maize cultivation. Settlement was restricted to several small hamlets  
187 close to, but outside the basin. A major change occurred around the year 2000 when  
188 an 'ecotourism' complex was established near the edge of the lake, with  
189 construction of buildings, infrastructure and landscaping.

190

191 3. Materials and Methods

192

193 Two parallel sediment cores were retrieved from 23.5 and 24.4 m water depth in  
194 Laguna de Juanacatlán in October 2003 using a Kullenberg system (Fig. 1b). The  
195 sediment-water interface was recovered simultaneously with a gravity corer  
196 attached to the trigger arm of the Kullenberg. MOLE-JUAN03-1A and -2A were 987  
197 cm long and 946 cm long respectively. Cores were recovered in polycarbonate liners  
198 of 70mm diameter, cut into section lengths  $\leq 150$ cm, transported to the LacCore  
199 Facility at the University of Minnesota and refrigerated at 4°C. Cores were scanned  
200 on whole- and split-core multisensory loggers, split in half lengthwise, and  
201 photographed with a DMT CoreScan Colour linescan camera. Lithological core  
202 descriptions were completed following LacCore protocols (Schnurrenberger, 2003)  
203 and used to create an initial composite sequence (splice) of 779 cm to avoid  
204 stratigraphic disturbances evident in the laminated sediments. Magnetic  
205 susceptibility was analysed on split cores at 0.5-cm resolution using a Bartington  
206 MS2E point sensor on a Geotek MSCL-XYZ automated core logger. The composite  
207 splice was sub-sampled into u-channels and scanned using an Itrax® XRF core  
208 scanner (Croudace et al., 2006) at Aberystwyth University at 200- $\mu$ m resolution, with  
209 settings at 30kV and 30mA and a 10-second count time. The chronology for the  
210 composite sequence is based on 26 AMS radiocarbon dates, with additional age  
211 control based on  $^{137}\text{Cs}$  peaks that correspond to weapons testing (1963 CE) and the  
212 Chernobyl nuclear accident (1986 CE). Details of the dates and age model are  
213 reported in Metcalfe et al. (2010) and Jones et al. (2015). A laminae count was based  
214 on visual inspection of the u-channel samples and the core photographs and the  
215 laminae types were classified based on both the visual stratigraphy and examination  
216 of example thin sections from each unit identified.

217

218 Samples were taken from the splice at 5-cm intervals for total organic carbon (TOC),  
219 total nitrogen (TN) and bulk organic carbon stable isotope ( $\delta^{13}\text{C}$ ) analysis. Sediment  
220 samples were washed in 5 % hydrochloric acid to remove calcite, rinsed in deionised  
221 water, dried at 40°C, then ground with an agate pestle and mortar. Carbon isotope  
222 measurements were carried out by combustion in a Carlo Erba 1500 on-line to a VG  
223 TripleTrap and Optima dual-inlet mass spectrometer.  $\delta^{13}\text{C}$  values were calculated to  
224 the VPDB scale using within-run laboratory standards. Replicate analysis of standard

225 materials indicated a precision of  $\pm 0.1 \text{ ‰}$  (1 SD) ( $n=37$ ). TOC and TN  
226 concentrations were measured as a by-product of the same process, calibrated  
227 against an Acetanilide standard. Replicate analysis of samples indicated a precision  
228 of  $\sim 0.4 \text{ ‰}$  (2 sigma).

229

230 Diatom species assemblages were analysed at 10-cm resolution through the  
231 composite sequence. Samples were digested in hydrogen peroxide using standard  
232 protocols described in Battarbee (1986), with aliquots mounted onto slides using  
233 Naphrax™ resin. Diatoms were counted at 1000x magnification using an Olympus  
234 BX50 microscope or a Zeiss Axioskop2 Plus microscope. At least 400 valves were  
235 counted for each sample and identifications were made with reference to published  
236 floras (Krammer and Lange-Bertalot, 1986, 1988, 1991a, 1991b; Gasse, 1986) and  
237 online databases (e.g. <https://westerndiatoms.colorado.edu/>).

238

239 We also report results of pollen analysis of a 900-cm core (JUAN-90-2) retrieved in  
240 1990 from 11.5 m water depth, using a Livingstone corer (Fig. 1b). Calibrated ages  
241 from six AMS  $^{14}\text{C}$  dates on plant fragments were used to create a linear age model to  
242 enable comparison with palaeoenvironmental data from the MOLE-JUAN cores.  
243 Pollen samples were taken at approximately 10-cm intervals, yielding a total of 93  
244 samples, and a known quantity of Lycopodium spores was added to each sample as a  
245 control. Pollen was extracted using standard techniques (Faegri and Iversen, 1989),  
246 including hydrochloric acid (10 %), KOH (10 %), hydrofluoric acid (49 %), nitric acid  
247 (50 %) and acetolysis. Residues were stained with safranin and mounted in silicone  
248 oil (2000 centistokes). In samples from diatom-rich levels, oil released during the  
249 hydrofluoric treatment often caused clumping at later stages of the extraction. This  
250 problem was minimized by washing with isopropanol immediately after the HF  
251 treatment, i.e., without an intervening water wash. The isopropanol wash was  
252 repeated several times if oil remained in the sample. After the final isopropanol  
253 wash, the sample was washed in water to avoid an explosive reaction with nitric  
254 acid. Pollen slides were counted on a Zeiss Photomicroscope with a 40x  
255 planachromat objective. Identifications were made with the aid of the University of  
256 California Museum of Paleontology Pollen Reference Collection and published keys

257 (Palacios-Chávez, 1968, 1985). The mean pollen count was 837, with a minimum of  
258 471. A total of 60 known pollen types were recognised and for most samples,  
259 unknowns accounted for less than 2% of the pollen sum.

260

## 261 4. Results and Interpretation

262

### 263 4.1 Stratigraphy and Chronology

264

265 The sedimentary sequence was largely laminated, consisting of greenish organic,  
266 diatomaceous layers with occasional fine-grained clastic layers. Five types of laminae  
267 were observed through the composite sequence (Fig. 2):

- 268 1. Organic laminae couplets of different shades, both with a clotted (ie.  
269 irregular, clumped) appearance.
- 270 2. Organic laminae couplets, one clotted, one not. Contained distinct, bright  
271 green laminae.
- 272 3. Dark brown and greenish-white non-clotted laminae.
- 273 4. Clotted organic laminae with fine-grained pink clastic laminae.
- 274 5. Non-clotted organic laminae with fine-grained pink clastic laminae.

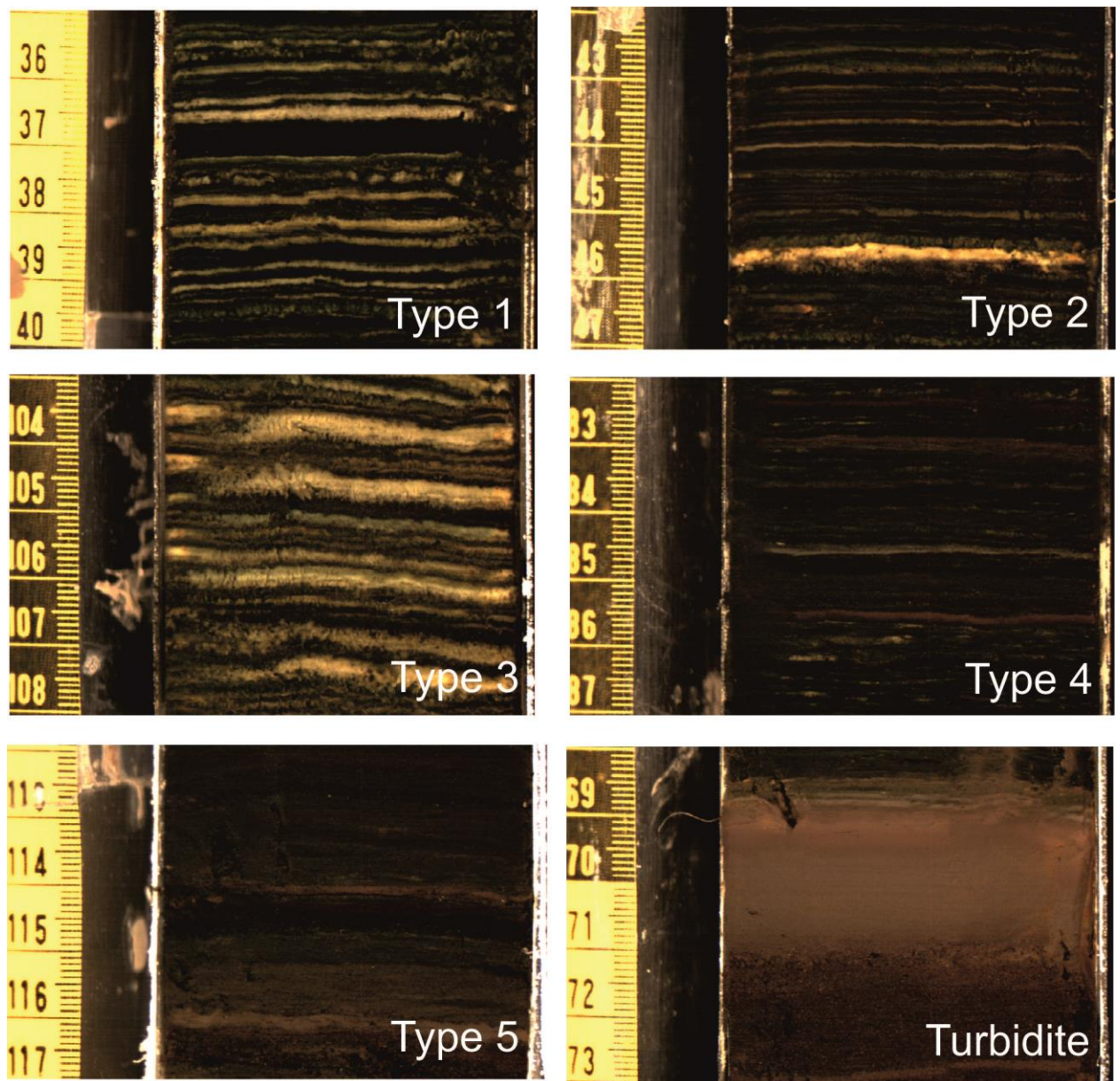
275

276 A total of 2732 laminae pairs were counted. The basal age of 5.79 cal ka for the  
277 sequence (Jones et al., 2015) implies that the laminae were not deposited annually,  
278 even considering that lamination was less clear in some sections of core. The  
279 composite sequence was divided into six units, characterised by laminae type. Unit 6  
280 (779-710 cm) was dominated by type 1 laminae. Unit 5 (710-445 cm) was dominated  
281 by type 3 laminae, which were about 2 – 3 mm thick. Unit 4 (445-265 cm) contained  
282 a mixture of clastic type 5 and entirely organic, type 3 couplets. Unit 3 (265-225 cm)  
283 was characterised by type 1 organic couplets. Unit 2 (225-17 cm) was dominated by  
284 type 4 and type 5 couplets. Unit 1 (0-17 cm) was dominated by type 1 organic  
285 couplets with a lower clastic content than Unit 2.

286

287 There were six non-laminated sections of different thicknesses, characterised by  
288 fining-upwards sequences, some with basal sands (Fig. 2; Table 1). These were

289 interpreted as turbidite deposits that represent instantaneous events, possibly  
290 related to tectonic or storm activity (Metcalf et al., 2010; Jones et al., 2015).  
291 Turbidites were removed from the composite sequence, consistent with our  
292 previous work, and given the focus here on identifying patterns of change over time.  
293 The final composite sequence was therefore 725 cm long.  
294



295  
296  
297 **Figure 2: Examples of the five laminae types identified in the MOLE-JUAN cores and**  
298 **an example of one of the turbidite layers (4 in Table 1) which were removed from**  
299 **the composite sequence for the purposes of this study.**

300

301 Table 1: Depth and age of turbidite layers in the MOLE-JUAN composite sequence.

302

<b>Turbidite</b>	<b>Upper depth (cm)</b>	<b>Lower depth (cm)</b>	<b>Age (cal ka)</b>
1	92	105.1	221
2	166.4	184.9	585
3	203.8	210	727
4	570	573.7	4231
5	601.6	613.6	4453
6	683.4	680.7	4912

303

304

305 The 900-cm Livingstone core (JUAN-90-2) retrieved in 1990, on which pollen analysis  
306 was performed, was moderately to well-laminated for most of the sequence. Non-  
307 laminated intervals were observed from 820 cm to the base and at 640-600, 450-430  
308 and 300 – 150 cm. A possible black tephra layer was found at 650 cm. A number of  
309 oxidised clay layers/flood deposits (turbidite layers) were also observed. These  
310 showed a similar pattern of distribution as the MOLE-JUAN sequence, with the  
311 turbidite layers in the upper 200 cm and below 450 cm depth. Radiocarbon dates on  
312 plant macrofossils (Table 2) were used to develop an age-depth model for JUAN-90-  
313 2, based on linear interpolation. Dates were calibrated using Intcal04 (Reimer et al.,  
314 2004), for consistency with the MOLE-JUAN chronology. The resulting basal age for  
315 the full sequence was 7.3 cal ka. Here we only present data from the last 6 cal ka, to  
316 provide temporal overlap with MOLE-JUAN.

317

318 Table 2: Radiocarbon dates from core JUAN-90-2 used to construct the linear age-  
319 depth model.

320

<b>Depth (cm)</b>	<b>Lab. Code</b>	<b><sup>14</sup>C yr BP</b>	<b>Cal yr BP (2σ)</b>
203	CAMS-27561	1140 ± 60	932 – 1228

288	CAMS-29428	2320 ± 50	2155 – 2655
490	CAMS-10223	3660 ± 45	3862 – 4144
678	CAMS-29426	5030 ± 60	5649 – 5910
694	CAMS-29430	5080 ± 60	5661 – 5796
873	CAMS-27559	5960 ± 80	6568 – 7138

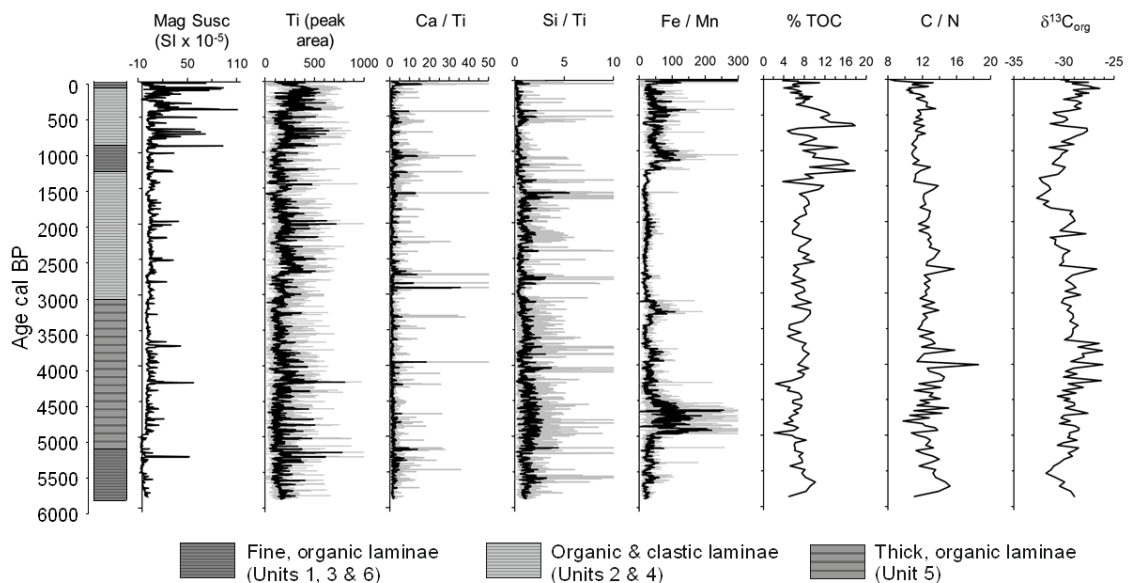
321

322

323 4.2 Magnetic Susceptibility and XRF scanning

324

325 Results of magnetic susceptibility and XRF core scanning are presented against age  
 326 for the MOLE-JUAN composite sequence (Fig. 3). Between 5.8 and 5 cal ka, magnetic  
 327 susceptibility values were at their lowest in the sequence, with frequent negative  
 328 values indicating diamagnetic properties of the sediment. Magnetic susceptibility  
 329 remained low between 4.95 and 1.0 cal ka, with a mean of  $4.4 \text{ SI} \times 10^{-5}$ . Notable  
 330 peaks, coinciding with increases in Ti, occurred at 5.2 and 4.2 cal ka, with smaller  
 331 peaks at 3.6, 2.8, 2.5, 2.1, 2.0, 1.9 and 1.2 cal ka. These all corresponded to pink clay  
 332 layers that were thicker than typical type 4 or 5 clastic/organic laminae couplets.  
 333 Higher magnetic susceptibility values were observed during the last 1.0 cal ka, with  
 334 mean values of  $12 \text{ SI} \times 10^{-5}$  and a series of large peaks between 60 and  $110 \text{ SI} \times 10^{-5}$ .  
 335



336

337

338 **Figure 3: Magnetic susceptibility, summary of XRF scanning and bulk organic**  
339 **geochemistry profiles for the MOLE-JUAN composite sequence. Numbers on the**  
340 **stratigraphic column refer to units described in section 4.1 based on dominant**  
341 **laminae type.**

342

343 Titanium (Ti) co-varied with magnetic susceptibility throughout the sequence. We  
344 previously established Ti as a proxy for catchment run-off related to rainfall  
345 (Metcalf et al., 2010; Jones et al., 2015). Some Ti peaks may represent individual  
346 inwash events. Other elements that would also be expected to represent  
347 allochthonous, minerogenic inputs, such as potassium, were strongly correlated with  
348 Ti ( $R^2 > 0.8$ ; Metcalf et al., 2010) and are not shown here.

349

350 In-lake processes can be explored by normalisation of key elements to Ti, which is an  
351 unambiguous indicator of external inputs. Ca/Ti ratios indicate authigenic processes  
352 such as evaporative concentration or biogenic calcite production (Davies et al.,  
353 2015). Both mechanisms are possible at Juanacatlán, a Ca Mg HCO<sub>3</sub> lake which could  
354 be expected to precipitate carbonate through evaporative concentration. Higher  
355 Ca/Ti ratios were observed at the base of the core, between c. 5.7 and 5.1 cal ka,  
356 with short-lived peaks centred around 3.2, 2.9, 2.7, 1.5 cal ka. In the upper part of  
357 the core, additional periods of higher Ca / Ti were evident, from 1.1 to 0.9 cal ka and  
358 from 0.6 to 0.4 cal ka, with another rise around 50 years ago.

359

360 Si/Ti ratios can be used to examine changes in biogenic silica, with increases in Si/Ti  
361 usually related to enhanced diatom productivity (Brown et al., 2007). The silica peak  
362 area values were low (mean < 110) and should be treated with caution. The 25-point  
363 moving-average data, however, showed generally higher values between 5.5 and 4  
364 cal ka and lower values over the last 3.0 cal ka. Peaks in the upper part of the core  
365 were observed from 2.8 to 2.6, 2.3 to 2.1, 1.6 to 1.5, 0.5 to 0.4 cal ka and in the last  
366 60 years.

367

368 Cluster analysis of downcore geochemical variations was previously carried out on  
369 the record of the last 2,000 years (Metcalf et al., 2010). This indicated that iron (Fe)  
370 was not consistently related to Ti and therefore unrelated to catchment inputs  
371 (Metcalf et al., 2010). Along with manganese (Mn), Fe can reflect changing redox  
372 conditions (Mackareth, 1966; Engstrom and Wright, 1984; Boyle, 2001). We explored  
373 this using the Fe/Mn ratio. Greater Fe/Mn indicates more reducing conditions at the  
374 sediment-water interface and enhanced lake stratification. Fe/Mn ratios were  
375 generally low between 5.8 and 1.26 cal ka, but punctuated by a significant increase  
376 between c. 5.0 and 4.4 cal ka. Smaller peaks were also observed between 3.9 and 3.7  
377 cal ka and 3.2 and 3.1 cal ka. Fe/Mn ratios increased after 1.3 cal ka, with a major  
378 peak in the last 60 years.

379

380 Catchment inputs, indicated by magnetic susceptibility and Ti values, were low  
381 through most of the sequence, but increased substantially after c. 0.9 cal ka. Earlier  
382 peaks occurred at c. 5.2 and 4.2 cal ka and more generally between 2.8 and 1.9 cal  
383 ka, but with less intensity than in the uppermost sediments. Peaks in Ca/Ti and Si/Ti  
384 ratios coincide, indicating that when biogenic silica production was higher,  
385 endogenic calcite production also increased. Si/Ti ratios (25-pt moving average) were  
386 generally higher in the lower part of the core, especially between 5.5 and 4 cal ka.  
387 This coincided with increased Fe/Mn ratios, indicating that increased biogenic silica  
388 production was associated with more reducing conditions and a stable catchment,  
389 the latter evidenced by low magnetic susceptibility and Ti values. Within the last 0.9  
390 cal ka, lake conditions appear to have been more variable, with periods of increased  
391 catchment inwash alternating with more reducing conditions and enhanced lake  
392 stratification.

393

#### 394 4.3 Bulk organic geochemistry

395

396 The ratio of carbon to nitrogen (C/N) in the organic component of lake sediments,  
397 combined with  $\delta^{13}\text{C}$  values of the organic matter, can provide information on the  
398 source of organic matter and the amount of biological productivity (Meyers and  
399 Lalliers-Verges, 1999). Bulk organic geochemical data are presented in Figure 3. The

400 variation in C/N ratios and  $\delta^{13}\text{C}_{\text{org}}$  values through the core was relatively small,  
401 indicating rather subtle changes in catchment vegetation and/or productivity  
402 (increased productivity can lead to higher  $\delta^{13}\text{C}_{\text{org}}$ ; Leng and Marshall 2004). Total  
403 organic carbon content (% TOC) of the sequence ranged from 2.1 % to 17.9 %.  
404 Percent TOC remained relatively stable through the core from 5.8 until 1.6 cal ka,  
405 fluctuating between 2.1 and 9.9 %, with a mean of 7 %. Between 1.6 cal ka and  
406 present, the mean increased to 8.9 %, with greater variability, from 3.9 to 17.9 %.  
407 Two distinct peaks in % TOC were observed between 1.2 to 0.9 cal ka and at c. 0.6 cal  
408 ka.

409  
410 C/N ratios were less variable, exhibiting a slight declining trend through the core. The  
411 C/N ratio of algae is generally between 4 and 10, and higher in terrestrial plants,  
412 usually > 20 (Meyers, 1994). The lower part of the sequence, between c. 5.8 and 3.4  
413 cal ka, was more variable than the most recent 3,000 years, with a return to  
414 increased variability in the last 150 years. Values in the MOLE-JUAN core ranged  
415 from 18.6 (at 3.9 cal ka), characteristic of mixed algal and terrestrial composition, to  
416 8.3 (core top), indicating an algal source.

417  
418 The sediments were diatomaceous throughout all the organic laminae, and it is  
419 therefore likely that diatoms were the main source of organic matter. No data are  
420 available on the  $\delta^{13}\text{C}$  composition of modern diatoms in Laguna de Juanacatlán, but  
421 algae (including diatoms) usually range between  $-20$  and  $-30$  ‰ (Galimov, 1995;  
422 Meyers and Teranes 2001). The  $\delta^{13}\text{C}$  of bulk organic matter from the sequence  
423 fluctuated between  $-26.4$  and  $-32.8$  ‰. Between 5.8 and 2.5 cal ka, the mean value  
424 was  $-29.3$  ‰, with a period of lower values between 5.6 and 5.3 cal ka, and  
425 increased variability between 4.6 and 3.6 cal ka. A trend towards lower values was  
426 observed after 2.5 cal ka, reaching about  $-32$  ‰ between 1.7 and 1.3 cal ka, before  
427 increasing again towards the top of the sequence. There is no indication in the  
428  $\delta^{13}\text{C}_{\text{org}}$  record of the presence of C4 plants, which typically have substantially higher  
429  $\delta^{13}\text{C}$  values than algae or C3 terrestrial plants (Meyers, 1994). A number of modern  
430 vegetation samples collected around the lake margins and catchment slopes have

431 values within the range of the sediments, including the emergent aquatic  
432 macrophyte *Juncus* (C/N 12;  $\delta^{13}\text{C}$   $-30.5$  ‰) and herbaceous *Salvia* (C/N 10.4;  $\delta^{13}\text{C}$   $-$   
433  $31.8$  ‰) (Aston, 2008). The predominance of C3 plants was confirmed by pollen  
434 analysis (see below).

435

436 Taking the % TOC, C/N and  $\delta^{13}\text{C}$  data together, four key periods can be identified. At  
437 the base of the core, between c. 5.8 and 5.1 cal ka, declining % TOC and C/N,  
438 combined with tendency towards higher  $\delta^{13}\text{C}_{\text{org}}$  values, suggest that algal sources  
439 were dominant and there was increasing productivity over this period. Between 5.1  
440 and 4 cal ka, % TOC remained stable, but C/N ratios and  $\delta^{13}\text{C}$  values co-vary and  
441 generally increase, with both reaching their highest values in the core. This is  
442 consistent with increased, but variable inputs from catchment sources. From 3.6 to  
443 1.3 cal ka, stable and slightly lower C/N ratios and  $\delta^{13}\text{C}_{\text{org}}$  point to an increased algal  
444 contribution to lake sediment organic matter. After 1.3 cal ka, the nature of the  
445 relationship between the sediment variables changed, indicating a shift in underlying  
446 causes. C/N ratios remained stable, indicating a consistent organic source, whilst %  
447 TOC and  $\delta^{13}\text{C}_{\text{org}}$  values were variable and anti-phased. Higher  $\delta^{13}\text{C}_{\text{org}}$  values, reaching  
448  $-26.4$  ‰, but stable C/N ratios, suggest increased algal productivity.

449

#### 450 4.4 Diatom assemblages

451

452 Diatom species assemblage data are summarised in Figure 4. The planktonic  
453 *Discostella stelligera* (Cleve and Grunow) Houk and Cleve, was common throughout  
454 the core, accompanied by a smaller form,  $< 5$   $\mu\text{m}$  in diameter, possibly *Discostella*  
455 *glomerata*, but it is problematic to distinguish when counting under light microscopy  
456 and is referred to as 'stelligeroid group ( $< 5$   $\mu\text{m}$ )'. Between c. 5.8 and 5.1 cal ka,  
457 *Discostella* species dominated the assemblage, mainly the larger *stelligera* type,  
458 accompanied by *Aulacoseira granulata* (Ehrenberg) Simonsen, making up to 20 % of  
459 the total. A distinctive feature of this period was the presence of *Fragilaria*  
460 *crotonensis* var. *oregona* Sovereign, with relative abundance up to 40 % at c. 5 cal ka.

461 *Urosolenia* spines were well preserved between 5.4 and 5.1 cal ka, their only  
462 occurrence in the record.

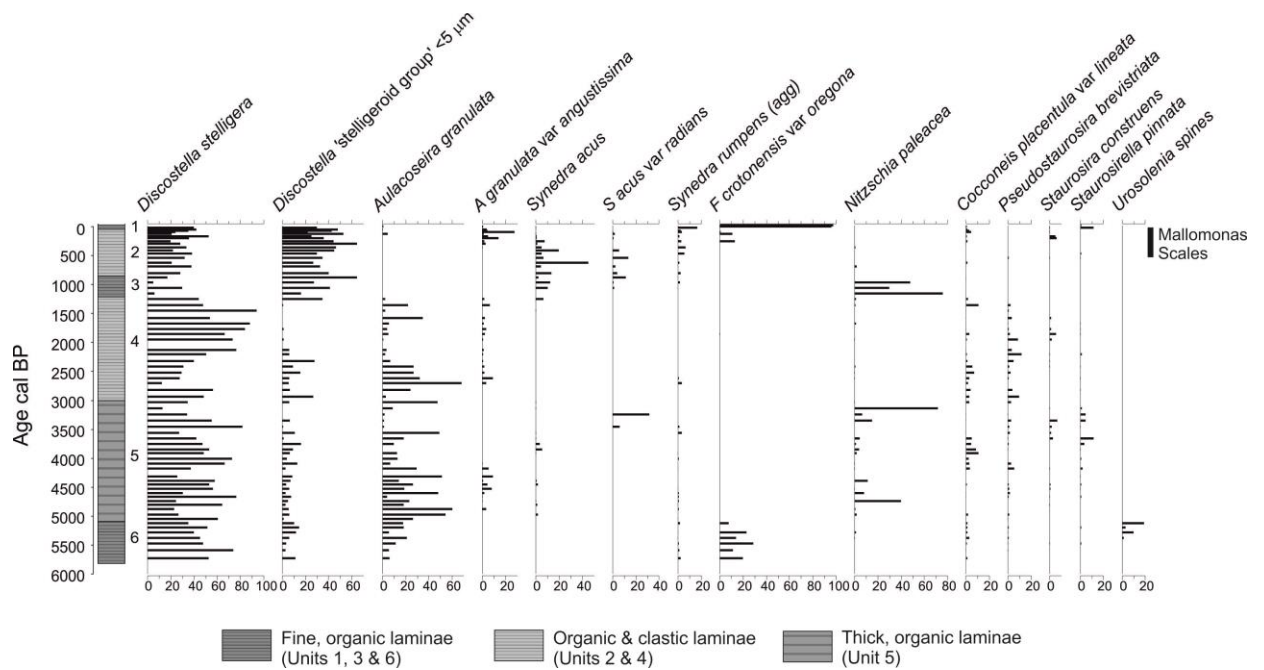
463

464 Between c. 5.1 and 1.2 cal ka BP, the diatom record continued to be dominated by  
465 *Discostella stelligera*, with *Synedra* species present in small amounts. The relative  
466 importance of *Discostella stelligera* and *Aulacoseira granulata* fluctuated through  
467 this period. A distinct peak of *Nitzschia paleacea* Grunow in Van Heurck occurred at  
468 c. 4.7 cal ka. Above this, *A. granulata* were present in higher numbers, up to 60 %,  
469 between 4.6 and 3.5 cal ka. The epiphytic species, *Cocconeis placentula* Ehrenberg  
470 also increased in abundance between c. 4.0 and 3.6 cal ka. A single peak of *S. acus*  
471 var. *radians* (Kützing) Hustedt was observed at 3.23 cal ka, followed by the  
472 reappearance of *N. paleacea* in large numbers at c. 3.1 cal ka. *A. granulata*  
473 increased in abundance between 3.0 and 2.4 cal ka. Two peaks of the small  
474 *Discostella* 'stelligeroid group' occurred at c. 2.9 and 2.3 cal ka.

475

476 Between 2.3 and 1.6 cal ka, *A. granulata* abundance was very low, rising again  
477 between 1.6 and 1.3 cal ka. A number of tychoplanktonic species were also present  
478 in low numbers through this period, including *Staurosirella pinnata* (Ehrenberg)  
479 Williams and Round, *Staurosira construens* Ehrenberg and *Pseudostaurosira*  
480 *brevistriata* (Grunow) Williams and Round. *Cocconeis placentula* was also present in  
481 small amounts, with a peak at 1.3 cal ka.

482



483

484

485 **Figure 4: Summary of diatom species assemblages from the MOLE-JUAN composite**  
 486 **sequence (species with at least 3% abundance are plotted).**

487

488 A notable shift in the diatom assemblage occurred during the last 1.2 cal ka.

489 Between 1.2 and 0.9 cal ka, *Nitzschia paleacea* dominated the assemblage at values  
 490 of up to 80 %, having been absent from the record for the previous 2,000 years.

491 Whilst *Discostella stelligera* was still present at values of c. 40 %, the proportion of  
 492 the smaller *Discostella* species increased substantially to between 30 and 60 % of the

493 total. *Synedra* species were also common, at values of 5 – 20 %. Over the last 300

494 years, the relative abundance of *Aulacoseira granulata* var. *angustissima* (Müller)

495 Simonsen reached its highest level in the sequence. Also present in diatom samples

496 over the last 500 years were abundant *Mallomonas* scales, tentatively identified as

497 *M. pseudocoronata* Prescott.

498

499 The most striking change in the entire MOLE-JUAN sequence was observed in the

500 uppermost sediments, where the dominant *Discostella* species were completely

501 replaced by monospecific blooms of *Fragilaria crotonensis* var. *oregona* in the last 20

502 – 30 years. *Mallomonas* scales were not found within these uppermost samples.

503

504 The diatom species in the MOLE-JUAN sequence do not reflect major changes in  
505 ionic concentration of lake waters, with the major taxa in the MOLE-JUAN sequence  
506 found in Mexican lakes with circumneutral to alkaline waters of low conductivity  
507 (Davies et al., 2002). The most common species in the core, *Discostella stelligera*, has  
508 been interpreted as an indicator of recent warming and enhanced lake stratification  
509 in Arctic and temperate environments (Rühland et al., 2015). Saros et al. (2012)  
510 found that nutrient availability also plays an important role in its response to  
511 changes in mixing depth. In Mexico, it has been found in deeper freshwater lakes of  
512 the volcanic highlands (Davies et al., 2002) and occurs in numerous Holocene and  
513 Late Pleistocene records from the region (Bradbury, 2000; Caballero et al., 2006;  
514 Metcalfe et al., 2007). In contrast, *Aulacoseira granulata*, a more heavily silicified  
515 diatom requires nutrient-rich, well-mixed waters to remain buoyant (Bradbury,  
516 2000). A diatom-based interpretation of limnological change is outlined for key time  
517 periods below, the forcing mechanisms behind which are considered in the  
518 synthesis.

519

520 Between 5.8 and 5.1 cal ka, dominance of *D. stelligera* over *A. granulata* suggests  
521 enhanced stratification and shallower mixing depth. *Fragilaria crotonensis* var.  
522 *oregona* is also present in substantial numbers. The ribbon-like chains formed by this  
523 species probably increases its ability to compete for nutrients (Rühland et al., 2015).  
524 *F. crotonensis* is widely acknowledged as an indicator of nutrient enrichment  
525 (Bradbury, 1975; Yang et al., 1996). The presence of delicate *Urosolenia* spines  
526 reflects exceptional preservation, indicating a very stable water column and high  
527 silica availability.

528

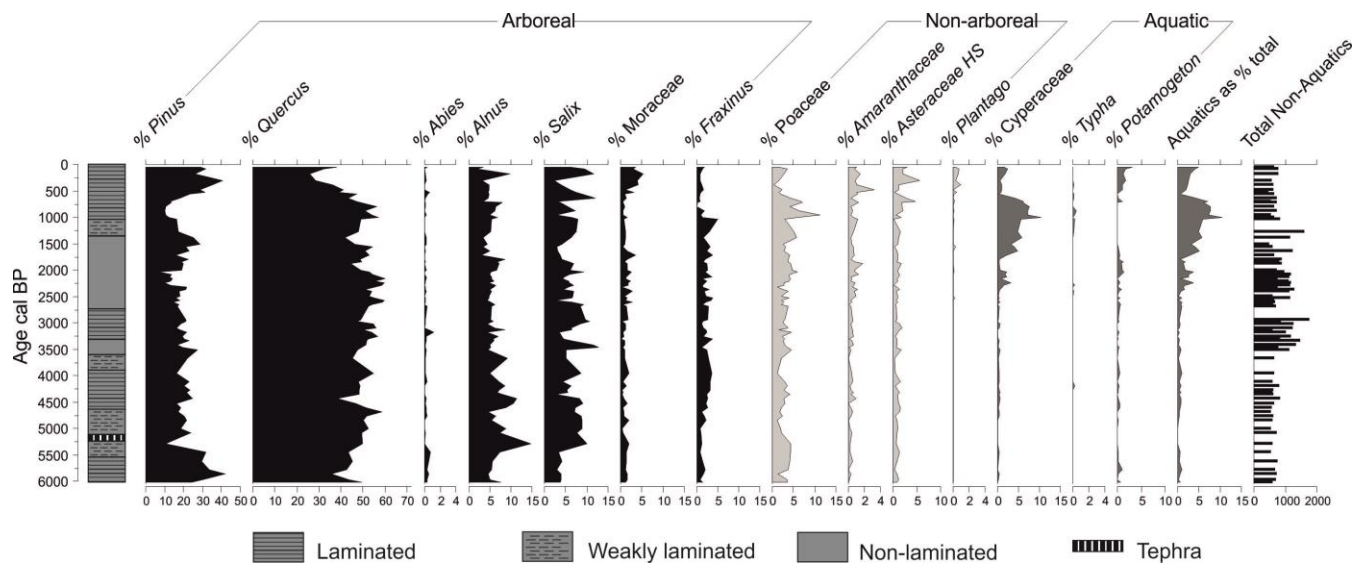
529 After 5.1 cal ka, the increase in *A. granulata* relative to *D. stelligera* suggests a  
530 change in the mixing regime to less well-stratified conditions or more regular  
531 overturning. Two distinct peaks in *Nitzschia paleacea* occur within this period (c. 4.74  
532 and 3.1 cal ka). Whereas these sudden increases may represent the tendency of this  
533 species to bloom (Woodbridge and Roberts, 2011), the samples averaged multiple  
534 laminations and these occur only in specific parts of the core. *N. paleacea* was  
535 associated with periphytic assemblages in modern samples from Laguna Zacapu

536 (Metcalf, 1988) and has been interpreted as indicating warm, alkaline and shallow  
537 conditions, representing less turbid waters than *A. granulata* (Metcalf, 1995).  
538 However, the water must have been deep enough to be stratified during these  
539 episodes. One explanation is that *N. paleacea* peaks may indicate periods of  
540 enhanced stratification, with increased phosphorus availability relative to silica  
541 (Kilham et al., 1986). After 2.3 cal ka, the return to dominance of *C. stelligera*, but  
542 lack of *A. granulata*, indicates continued stratification, with further intensification of  
543 these conditions between 1.2 and 0.9 cal ka inferred from another *N. paleacea* peak.  
544 After 0.9 cal ka, the increase in *Synedra* species suggests a further shift in nutrient  
545 availability. Kilham et al. (1986) demonstrated that *Synedra* spp. are more effective  
546 competitors in systems with a limited phosphorus supply, and reflect high Si/P ratios.  
547 The peak in abundance of *Aulacoseira granulata* var. *angustissima* after 0.2 cal ka  
548 represents a shift to this morphological form instead of the nominate variety. The  
549 reason for this is difficult to interpret as the two forms have similar ecological  
550 requirements, although the rise in numbers of this genus does indicate increased  
551 turbidity. The very recent and dramatic change in the diatom assemblage to one  
552 entirely dominated by *Fragilaria crotonensis* var. *oregona* was previously interpreted  
553 in short cores as a response to recent anthropogenic disturbance in the catchment  
554 and associated eutrophication (Davies et al., 2005). The nominate variety is known to  
555 compete well where nitrogen concentrations are increased relative to phosphorus  
556 (Saros et al., 2005, 2011), and could indicate both local and regional signals.  
557 Nevertheless, because this species is also found at the base of the core, prior to the  
558 likely influence of human activities, natural drivers probably produced favourable  
559 conditions for this species during the Holocene.

560

561 4.5 Pollen assemblages

562



563

564

565 **Figure 5: Summary pollen diagram for Core JUAN-90-2.**

566

567 Pollen data from JUAN-90-2 are plotted as percentages of the total pollen sum in Fig.

568 5. Although aquatic pollen are sometimes excluded from the total, here they

569 generally account for < 5 % of the total, except for the interval between about 1.3

570 and 0.65 cal ka when there are higher percentages of Cyperaceae. As the inclusion

571 of aquatic pollen makes little difference to the percentages of non-aquatic pollen

572 types, here we include them in the total pollen sum. *Pinus* (pine) and *Quercus* (oak)

573 account for between 52% and 77 % of the total pollen sum in JUAN-90-2. Before c.

574 5.4 cal ka, *Pinus* and *Quercus* are co-dominant (together > 70 %), with low

575 percentages of other tree species such as *Alnus* (alder) and *Salix* (willow). Grasses

576 and herbs comprise a low percentage of the total pollen count. Between c. 5.4 and

577 0.5 cal ka, oak is present at higher percentages than pine. The pollen assemblage

578 through this interval is marked by higher percentages of alder (up to 14.8 %) and

579 willow (up to 12.8 %). From about 2 cal ka there is an increase in pollen percentages

580 of emergent aquatic plants, including *Typha* (cattails), and Cyperaceae (sedges),

581 which reach 10.4 % of the total pollen count at 0.95 cal ka. The top part of the core

582 is marked by a switch back to pine > oak, with a clear increase in Moraceae (up to 5.3

583 %), a group that includes *Ficus* and *Morus* (Ramos Zamora, 1977). Amongst the non-

584 arboreal pollen, there are increases in high-spine Asteraceae and *Plantago*. In the

585 aquatic pollen, there is a decline in Cyperaceae and *Typha* and an increase in

586 *Potamogeton* (pond weed), which forms 3.2 % of the total pollen sum at the top of  
587 the core.

588

589 The interpretation of the pollen evidence from the highlands of Central Mexico has  
590 been complicated because of the dominance of taxonomically difficult taxa such as  
591 pine, oak, and alder, and the overlapping effects of climate change, human-induced  
592 disturbance and volcanic activity. Different species of pine and oak form different  
593 communities that occupy rather different environments with respect to moisture  
594 availability and temperature, but are difficult to distinguish using standard  
595 palynological techniques (Lozano García and Xelhauntzi Lopez, 1997; Lozano-García  
596 and Ortega-Guerrero, 1998). They also produce very large amounts of pollen. In  
597 contrast, *Abies* (fir), which may be a component of these pine-oak forests  
598 (increasingly so at higher elevations), has low pollen productivity and may be under-  
599 represented by its pollen (Watts and Bradbury, 1982; Lozano-García, 1989). The  
600 changing ratios of pine and oak, or pine to oak + alder + fir, have been used in  
601 Mexican pollen studies to try and elucidate the nature of past climate.

602 Unfortunately, interpretations of these ratios, and of switches between pine and oak  
603 more generally, have not been consistent (Deevey, 1944; Sears, 1952; Watts and  
604 Bradbury, 1982; Ortega Rosas et al., 2008; Park et al., 2010; Lozano-García et al.,  
605 2013).

606

607 The early part of the pollen record (prior to about 5.4 cal ka) indicates a catchment  
608 dominated by pine-oak woodland. Fir reaches its highest percentage in the last 6000  
609 years, but is still under 1%. *Salix* and *Alnus* are often found as riparian taxa in the  
610 Mexican volcanic highlands (Lozano-García et al., 2013) and their limited presence  
611 here may reflect a lack of suitable habitat when the lake was higher than it is today.  
612 After about 5.4 cal ka, there is a distinct decline in the percentage of pine, while the  
613 percentage of oak remains fairly stable (40 – 50 %). Such high percentages of oak  
614 pollen are rarely recorded in the TMVB, but have been recorded further north  
615 (~28°N) in the Sierra Madre Occidental (Ortega-Rosas et al., 2008). Although aquatic  
616 pollen remains poorly represented until about 2.5 cal ka, this part of the pollen  
617 diagram is marked by clear increases in alder and willow and a slight increase in

618 *Fraxinus* (ash). *Fraxinus* is described by Rzedowski (1994) as riparian or occupying  
619 valley bottoms in oak woodlands. This increase suggests a slight decline in lake level,  
620 which would have created a wider riparian zone, although the continuously  
621 laminated sediments throughout this part of the JUAN-90-2 core would seem to  
622 indicate at least 7-8 m of water at the coring site, based on comparison with a core  
623 taken in 7.35 m depth in 1990 but not analysed in detail. That core, like JUAN-90-2  
624 also preserved laminations in the surface and recent sediments. This depth is also  
625 consistent with measured thermocline depths (see above). It has been suggested  
626 that increasing predominance of oak relative to pine can be a result of succession, a  
627 more dominant summer precipitation regime or warming (Figueroa-Rangel et al.,  
628 2008; Ortega-Rosas et al., 2008; Correa-Metrio et al., 2012). Park et al. (2010)  
629 suggested that percentages of oak + alnus > pine (as here) are indicative of wet  
630 conditions. After about 2.5 cal ka, the arboreal pollen record remains stable, but  
631 there is a clear increase in the percentage of Cyperaceae (sedge) to a maximum of >  
632 10% of total pollen about 0.9 cal ka. Although sedges can grow in a wide range of  
633 habitats, these emergent aquatics have been reported as being very common  
634 around lakes in the TMVB (Bonilla-Barbosa and Novelo Retana, 1995). The  
635 expansion of sedges and the switch from laminated to unlaminated sediments in  
636 core JUAN-90-2 seem to indicate a fall in lake level and hence drier conditions. The  
637 peak in Poaceae (grasses) at about the same time, may confirm this. After about 0.9  
638 cal ka an increase in high-spine Asteraceae and the presence of large (> 80 µm)  
639 Poaceae (possibly *Zea mays* (maize), although not recorded as such) may indicate  
640 anthropogenic catchment disturbance. More distinct changes in the pollen record at  
641 about 0.5 cal ka, when there is an increase in Moraceae (up to 5.3%), persistently  
642 higher percentages of Amaranthaceae, and an increase in *Plantago*, seem to confirm  
643 this interpretation. High-spine Asteraceae and *Plantago* have both been interpreted  
644 as indicators of human disturbance (Almeida-Lenero et al., 2005; Bhattacharya et al.,  
645 2015). Amongst the Moraceae, *Ficus* are particularly common in this part of Mexico  
646 and many occur in moderately to strongly disturbed sites (Serrato et al., 2004).  
647 Moraceae in general and *Ficus* in particular, are also found mainly in warm and wet  
648 climate zones in Mexico. At the same time as this disturbance occurs, pine recovers  
649 to the percentages found near the base of the sequence, Cyperaceae declines, and

650 the submerged aquatic/floating mat-forming *Potamogeton* becomes more  
651 abundant. Taken together with a return to the deposition of laminated sediments in  
652 JUAN-90-2, it seems possible that the catchment was experiencing both more  
653 disturbance and higher water levels, although percentages of willow remain quite  
654 high.

655

## 656 5. Discussion

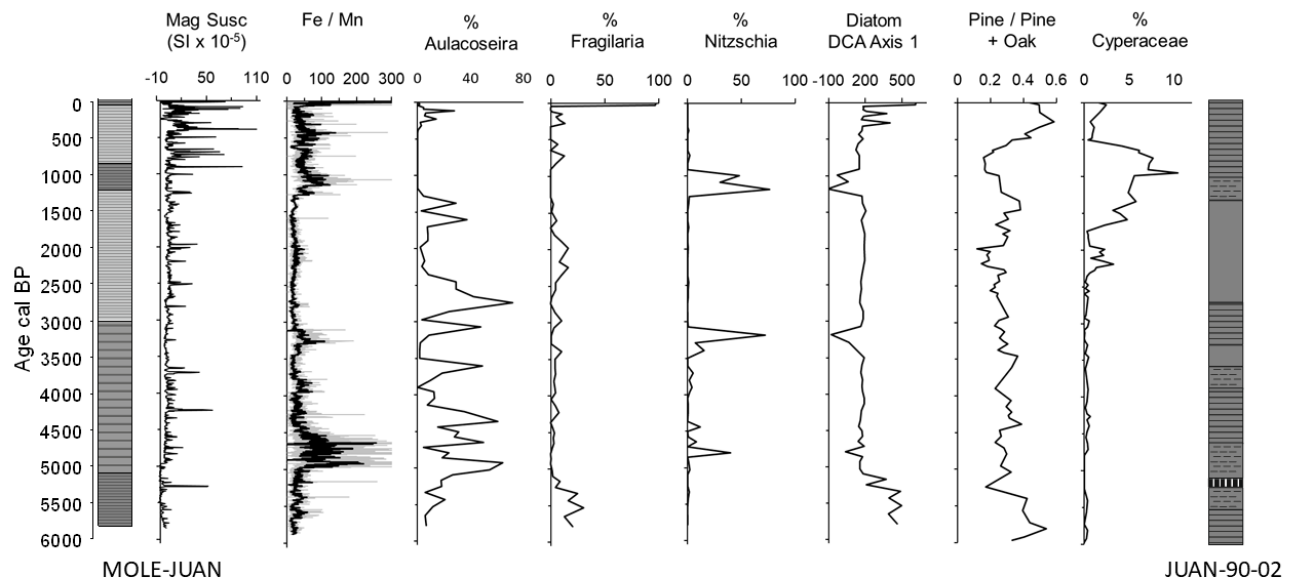
657

### 658 5.1 Palaeoenvironmental synthesis

659

660 Proxy palaeoenvironmental data from Laguna de Juanacatlán demonstrate variations  
661 in the mixing regime of the lake over the last 5.8 cal ka. This may have been caused  
662 by changes in water depth, temperature and wind speed, or a combination of these,  
663 but individual sediment variables cannot be used readily to identify which factors  
664 were responsible at any one time. Here, we synthesise the multiple sediment  
665 variables (Fig. 6) for key time periods and consider the likely forcing mechanisms  
666 behind the observed limnological and catchment changes. Detrended  
667 Correspondence Analysis (DCA; Hill and Gauch, 1980) was used to explore the  
668 environmental gradients in the pollen and diatom datasets.

669



670

671

672 **Figure 6: Summary of palaeoenvironmental data from the MOLE-JUAN composite**  
 673 **sequence and core JUAN-90-2 pollen analysis.**

674

675 5.1.1 ~ 5.8 to 5.1 cal ka

676

677 This period is characterised by low catchment inputs, with type 1 organic laminae  
 678 couplets. The diatom assemblage, represented by *D. stelligera* with *F. crotonensis*  
 679 var *oregona*, indicates a stratified and stable water column and mesotrophic  
 680 conditions that were similar to present. High positive scores on Diatom DCA Axis 1  
 681 (eigenvalue 0.64) during this period are driven by *F. crotonensis* var *oregona*. This  
 682 taxon was encountered previously only in the uppermost sediments at this site and  
 683 suggests high nitrogen concentrations relative to phosphorus and silica. Algae were  
 684 the main source of organic matter, with  $\delta^{13}\text{C}$  values suggesting an increasing trend in  
 685 lake productivity. Pollen DCA Axis 1 (eigenvalue 0.038) mirrored the pine profile (and  
 686 pine/pine +oak ratio) through the sequence and is therefore not presented. Up to c.  
 687 5.3 cal ka, pollen data point to wetter conditions, with increased pine/pine + oak  
 688 ratios and the presence of *Abies* at its highest concentrations in the sequence (but  
 689 still in low numbers). Together, these data suggest that generally moist conditions

690 maintained relatively high water levels and stable lake stratification. Some  
691 catchment disturbance around 5.2 cal ka, with higher Ti and magnetic susceptibility  
692 values, marks a change in the record after this point.

693

694 5.1.2 ~ 5.1 to 4.0 cal ka

695

696 This period is marked by the onset of more variable conditions, with episodic periods  
697 of catchment instability and an increase in C/N to its highest levels in the entire  
698 record, indicating increased inputs of higher plant material into the lake. The  
699 predominant laminae type changed in the deeper water core and in the shallower  
700 water core sediments changed from laminated to weakly laminated sediments. The  
701 increasing abundance of riparian vegetation (willow and alder, Fig. 5) probably  
702 indicates a lowering of lake level, consistent with the change in lamination at this  
703 site. The increasing importance of the diatom *A. granulata* and high Si:Ti indicate  
704 productive, silica rich conditions. Warm conditions could account for the  
705 predominance of oak in the terrestrial vegetation, periodic intense stratification  
706 (high Fe:Mn) and high levels of *N. paleacea*, particularly at ca. 4.7 cal ka (Figs 4 & 6).

707

708 5.1.3 ~ 4.0 to 1.2 cal ka (2050 BCE – 750 CE)

709

710 This continues the general drying of the earlier period. Catchment conditions appear  
711 to have been generally stable until around 3.0 cal ka. After this, there is an increase  
712 in sediment inputs from the catchment. The change to clastic laminae in the deeper  
713 water core confirm this trend. Shallower water is indicated by an increase in the  
714 proportions of epiphytic and periphytic diatoms (small Fragilaroid taxa, *C. placentula*;  
715 Fig 4) and the deposition of unlaminated sediments in the shallower water core.  
716 Willow and alder remain important components of the pollen flora, while towards  
717 the end of this period there is a marked increase in aquatic pollen, (e.g. Cyperaceae)  
718 possibly indicative of further shallowing (Figs 5 & 6).

719

720 5.1.4 ~ 1.2 to 0.9 cal ka (750-1050 CE)

721

722 The represents a brief period of catchment restabilisation, with a lack of clastic  
723 laminae at the deeper water site. The diatom record shows the last peaks of *N.*  
724 *paleacea* indicated by a shift to negative values on Diatom DCA Axis 1 and the start  
725 of higher proportions of *Synedra* spp (Diatom DCA Axis 2). *Nitzschia* species have  
726 been linked with increased nutrient availability from cyanobacteria which would be  
727 consistent with higher productivity indicated by the increase in % TOC and  $\delta^{13}\text{C}_{\text{org}}$   
728 values (Fig. 3). Cyperaceae continues to increase through this period. We interpreted  
729 the Ti record as an indicator of drier conditions (Metcalf et al., 2010; Jones et al.,  
730 2015). The signal from the palaeoecological evidence however is less clear. *N.*  
731 *paleacea* likely indicates warmer conditions and has been associated with lake  
732 shallowing in central Mexico (Metcalf, 1995). However, the return from non- to  
733 weakly-laminated sediments in core JUAN-90-2 does not support a lake level decline.  
734 The major change in the diatom flora does indicate a substantial change in  
735 limnological conditions and may be representing intensified stratification due to  
736 warming rather than any significant lake level lowering.

737

738 5.1.3 ~ 0.9 to –50 cal ka (1050 – 2000 CE)

739

740 Following the period of drier conditions which ends at c. 0.9 cal ka (1050 CE), a  
741 switch to higher values of magnetic susceptibility and Ti indicates a substantial  
742 increase in catchment inputs. Clastic laminae dominate in the MOLE-JUAN core. The  
743 generally greater catchment inwash is punctuated by periods of lower catchment  
744 inputs, between 0.6 and 0.4 cal ka (1350 – 1550 CE) and from 0.3 to 0.1 cal ka (1680 -  
745 1850). Within these time periods are several known historical multi-year droughts  
746 that are associated with lower Ti values (Metcalf et al., 2010). There is a substantial  
747 shift in the JUAN-90-2 pollen record over the last 0.9 cal ka, with pine increasing to  
748 its highest percentages. Oak is still common, at 30 % of the count, higher than in  
749 many other central Mexican sequences. Forest elements clearly remain dominant,  
750 but the increase in Poaceae, which begins around 0.9 cal ka, high-spine Asteraceae  
751 and Moraceae indicate anthropogenic disturbance of the catchment vegetation. This  
752 is the first clear signal of human influence in the record. The increase in pine over the  
753 last 500 years could be interpreted as a shift to wetter conditions, with similar

754 conditions to those prior to 5.3 cal. ka. This is also combined with a drop in  
755 Cyperaceae and higher abundance of *Potamogeton*, suggesting a modest increase in  
756 water level. Diatom DCA Axis 2 scores are higher, which reflects a shift towards the  
757 dominance of the smaller form D. 'stelligeroid group' and also an increase in *Synedra*  
758 species. Laminated sediments at both core sites suggest increased water depth. A  
759 switch from the presence of *Synedra* species to *Aulacoseira granulata* var.  
760 *angustissima* around 300 years ago, suggests increased mixing after this point,  
761 related to the combined influences of catchment disturbance and wetter conditions.  
762 The very recent and dramatic change to the diatom flora recorded since the 1990s,  
763 to a total dominance of *F. crotonensis* var *oregona* (high DCA Axis 1 scores; Fig. 6)  
764 signals a further strengthening of stratification and an increase in concentrations of  
765 nitrogen relative to phosphorus. Fine organic laminae dominate in the MOLE-JUAN  
766 core. We interpret this as a local anthropogenic signal, but there may also be a  
767 broader, regional influence from nitrogen deposition and anthropogenic warming.  
768 Combined impacts of ENSO events and recent warming have been linked to  
769 phytoplankton changes in a central Mexican crater lake (Caballero et al., 2016)  
770 Further high-resolution sampling resolution of surface cores and detailed  
771 limnological monitoring at Juanacatlán could be used to investigate these  
772 relationships further.

773

## 774 5.2 Implications for Holocene monsoon variability

775

776 The data presented here cover the period after the peak intensity of the North  
777 American Monsoon, which occurred around 6 cal ka (Metcalf et al., 2015). The  
778 transition from relatively wet to drier conditions begins c. 5.1 cal ka intensifying after  
779 c. 4.0 cal ka and is consistent with the weakening of the NAM as the ITCZ moved  
780 south. A number of records across Mexico indicate variable conditions between 6  
781 and 5 cal ka BP, as the declining influence of orbital forcing led to increased  
782 prominence of other forcing mechanisms (Metcalf et al., 2000). The timing of the  
783 transition to a weaker monsoon is consistent with records across the TMVB  
784 indicating a shift to drier conditions around 4 cal ka (Bernal et al., 2011, Lozano  
785 García et al., 2013; Metcalf et al., 2015).

786

787 An increase in the influence of ENSO and greater hydrological variability is inferred at  
788 several sites beginning c. 4 cal ka, including Pátzcuaro (Metcalfe et al., 2007) and  
789 Zirahuén (Ortega et al., 2010; Vázquez-Castro et al., 2010; Lozano et al., 2013)  
790 (Figure 1a). At Juanacatlán, dominance of a 20-25 year cycle in the Ti record after 3  
791 cal ka was interpreted as an increasing Pacific influence (Jones et al., 2015). This is  
792 reflected in the stratigraphy of the JUAN-MOLE composite as clastic laminae become  
793 common in Unit 4 (Fig 3). The palaeoecological record at Juanacatlán is of insufficient  
794 resolution to capture the decadal variability observed in the high resolution Ti record  
795 but does indicate a shift to drier and more variable conditions. Increasingly distinct  
796 fluctuations in moisture availability are also observed at some TMVB lakes, such as  
797 those in the Valle de Santiago (Park et al., 2010) over the late Holocene. The more  
798 intense human occupation history at sites like Pátzcuaro (Metcalfe et al., 2007) and  
799 Zirahuén (Lozano-García et al., 2013) probably sensitized the catchment response to  
800 hydrological changes, making it difficult to interpret the recent parts of these records  
801 strictly in terms of climate variability, at least compared to the pre-disturbance parts  
802 of the sequences.

803

804 We interpret the changes observed in the Juanacatlán record between 1.2 and 0.9  
805 cal ka (750 – 1050 CE) as indicating generally drier and warmer conditions. However,  
806 the record at this point may also reflect reduced rainfall variability and / or intensity,  
807 given the absence of any clastic laminations. The regional picture at this time is  
808 complex. Drier conditions are observed a little earlier than at Juanacatlán in high-  
809 resolution records from southwest Mexico. The Juxtlahuaca speleothem shows the  
810 onset of drought at 1.25 cal ka (~ 700 CE), peaking at 750 CE ('Epiclassic Drought'),  
811 with a switch to wetter conditions (Postclassic Pluvial) associated with increased La  
812 Niña influence (Lachniet et al., 2017). At Laguna Minucúa drought conditions are  
813 inferred between 1.28 and 1.16 cal ka (670 – 790 CE), followed by variable but  
814 wetter conditions. The laminated sequence from Santa Maria del Oro, north of  
815 Juanacatlán captures drought conditions between 1.5 and 1 cal ka (450 – 950 CE).  
816 The most intense phase, between 1.35 and 1.15 cal ka (600 - 800 CE) (Rodríguez  
817 Ramírez et al., 2015), peaks earlier than at Juanacatlán. The distinct period of

818 reduced run-off at Juanacatlán coincides with records elsewhere across  
819 Mesoamerica, which record prolonged drought conditions, the so-called Terminal  
820 Classic Drought (Hodell et al., 1995; 2005; Douglas et al., 2015), also clearly  
821 expressed across the TMVB (Metcalf et al., 1991; Metcalfe and Davies 2007;  
822 Bhattacharya et al., 2015).

823

824 Previous work suggested that the intense dry phase observed across Mesoamerica  
825 was caused by a shift in the strength and position of the Bermuda-Azores High and  
826 related to southward movement of the ITCZ (Metcalf et al, 2000). Recent modelling  
827 confirms a strong North Atlantic imprint on drought across the region, with a  
828 positive North Atlantic Oscillation (Bhattacharya et al., 2017), whilst in the Pacific  
829 Ocean, La Niña-like conditions prevailed during the Medieval Climate Anomaly  
830 (Metcalf et al., 2015). Lachniet et al. (2017) emphasise the complex interactions  
831 between East Pacific (ENSO) and Atlantic (NAO) forcings that are probably involved.  
832 Persistent La Niña conditions brought drier conditions to the region north of  
833 Juanacatlán but increased rainfall to the south (Metcalf et al., 2015). One possibility  
834 is that the catchment stability observed at Juanacatlán between 1.2 and 0.9 cal ka  
835 linked more closely to reduced rainfall variability rather than absolute values as  
836 lower Pacific sea surface temperature would result in fewer tropical storms. This  
837 period also coincides with reduced ENSO frequency recorded in the sediments of El  
838 Junco Lake in the Galapagos (Conroy et al., 2008).

839

840 The major shift in the diatom assemblage to *N. paleacea* dominance between 1.2  
841 and 0.9 cal ka was also observed earlier in the record, at 4.7 cal ka and 3.1 cal ka.  
842 These may also represent equivalent periods of drying / catchment stability and also  
843 coincide with low ENSO frequency in the El Junco record (Conroy et al., 2008).  
844 Comparison with other lakes in the TMVB is problematic for these two earlier *N.*  
845 *paleacea* phases as other records lack sufficient chronological resolution. Caballero  
846 et al. (2002) report a dry phase at Sta Cruz Atizapan at c. 4.5 cal ka, but timing of dry  
847 episodes at Zirahuén and Pátzcuaro in Michoacán only coincides with the 1.2-0.9 cal  
848 ka phase (Davies et al., 2004; Metcalfe et al., 2007; Ortega et al., 2010). More high

849 resolution lacustrine sequences extending back to the mid-Holocene are needed to  
850 explore these earlier episodes.

851

852 The Juanacatlán record fits the model of a two-part Medieval Climate Anomaly  
853 (Rodysill et al., 2018). The phase discussed above between 1.2 and 0.9 cal ka (750 -  
854 1050 CE) is quickly followed by a shift to substantially wetter conditions, although  
855 this signal may be enhanced by the onset of anthropogenic disturbance. The climate  
856 of the Little Ice Age (1400 – 1850 CE) also varied across the region, with a continued  
857 shift to markedly wetter conditions than during much of the record, but punctuated  
858 by drier periods corresponding to historic droughts (Metcalf et al., 2010).

859 Increasing regional variability during the last few hundred years is evident from a  
860 regional synthesis of records (Metcalf et al., 2015). Drier conditions between 0.6  
861 and 0.35 cal ka (1350 and 1600 CE) and the earlier one at 1.2 – 0.9 cal ka (750 – 1050  
862 CE) are antiphased with the Juxtlahuaca speleothem record (Lachniet et al., 2012;  
863 2017), but in phase with the nearest lake record at Santa Maria del Oro (Sosa Najera  
864 et al., 2010; Rodríguez Ramírez et al., 2015). The lake and cave records have  
865 different levels of chronological resolution, but may also record different aspects of  
866 the climate system (Lachniet et al., 2017). The position of Juanacatlán at the  
867 boundary between northern and southern regions in relation to Pacific forcings adds  
868 to the complexity.

869

870 5.4: Human – environment interactions

871

872 The timing of the onset of human disturbance varies across central Mexico, and it  
873 has been suggested it could be as early as 5.7 cal ka in southern Guanajuato (Park et  
874 al., 2010), whilst in the Cuenca Oriental in eastern Mexico, charcoal and pollen  
875 indicate an onset of agriculture c. 2.7 cal ka (Bhattacharya and Byrne, 2016). Here, at  
876 Laguna de Juanacatlán, we see no clear evidence of human activity until much later  
877 than at many other sites, after the drought event between 1.2 and 0.9 cal ka. The  
878 peak in Poaceae at the end of the drought may be related to anthropogenic  
879 disturbance, but could also be a response to the drier conditions. Given that it occurs

880 as the JUAN-90-2 core site becomes laminated again, signalling increased water  
881 depth, anthropogenic disturbance is the more likely explanation.

882

883 The evidence from Juanacatlán suggests that there was some minor forest clearance  
884 and cultivation in the basin during the Postclassic, but that human influence here  
885 was considerably less intense than observed at other sites across the TMVB  
886 (Metcalf et al., 2007; Lozano et al., 2013). There is currently no archaeological  
887 evidence to support dense settlement in the area (see section 2). This highlights the  
888 rare value of the palaeoecological record from Laguna de Juanacatlán, which  
889 primarily reflects a response to climate forcing during the late Holocene.

890

891 One topic of contentious debate is the relative amount of disturbance caused by pre-  
892 and post-Hispanic populations in central Mexico (Denevan, 1992; O'Hara et al., 1993;  
893 Fisher et al., 2003). At Laguna de Juanacatlán, the minor change in forest  
894 composition began c. 1200 CE prior to the Colonial Period (1521 CE) and probably  
895 represents the combined influences of climate change and human activity. The two  
896 small peaks in disturbance indicators at c. 1300 CE and 1700 CE are similar in  
897 magnitude. There is no evidence from the Juanacatlán catchment to indicate a more  
898 intense phase of human activity following the Spanish Conquest, despite historical  
899 records of mining activity during the 17<sup>th</sup> century in the area (see section 2.1).

900

901 The most pronounced anthropogenic signal occurs within the last 30 years, with a  
902 complete change in the diatom flora of the lake, which persisted through the most  
903 recent phytoplankton sampling in 2011 (Sigala et al., 2017). This change in  
904 assemblage occurred prior to the establishment of a tourist complex on the lake  
905 shore. We previously interpreted this as a response to local catchment changes  
906 (Davies et al., 2005). The dramatic change, however, is consistent with evidence  
907 from alpine lakes in North America that phytoplankton have responded to increased  
908 atmospheric nitrogen deposition and anthropogenic warming (Saros et al., 2005;  
909 Rühland et al., 2015). Information from tropical lakes on the impact of these multiple  
910 stressors on phytoplankton composition is lacking. One problem is that it is difficult  
911 to disentangle these larger-scale driving mechanisms from local, catchment-scale

912 impacts. Rapid turnover of the diatom flora has also been observed in recent  
913 decades at Lago de Zirahuén (Davies et al., 2004) and Laguna Zacapu (Leng et al.,  
914 2005), but these have much more intense human activity around the basin and at  
915 the lake shore, and so probably represent local changes. One possibility is that  
916 recent warming effects are more visible at Laguna de Juanacatlán, in light of the  
917 muted magnitude of human impacts. A short core retrieved in 2003 from high-  
918 altitude Lake La Luna on the Nevado de Toluca, the same year as MOLE-JUAN,  
919 showed no evidence of recent, rapid change (Cuna et al., 2014), but Lake La Luna is  
920 an oligotrophic lake at a substantially higher altitude and may not have reached a  
921 threshold to initiate a nutrient-related response.

922

## 923 6.1. Conclusions

924

925 The palaeolimnological record from Laguna de Juanacatlán provides new insights  
926 into the links between climate variability and lacustrine response over the last c.  
927 6,000 years in western Mexico. The broad sequence of change is consistent with  
928 patterns observed at other sites in the Trans-Mexican Volcanic Belt. Less intense  
929 anthropogenic disturbance was evident here over the late Holocene, compared with  
930 other basins, suggesting that more subtle limnological responses to climatic change  
931 can be identified.

- 932 • Humid conditions, similar to present, are identified between 5.8 and c. 5.1 cal  
933 ka, with dense oak-pine forest, a deep, stratified lake and low catchment  
934 inputs.
- 935 • A transition to lower lake levels from 5.1 – 4.0 cal ka was observed, with drier  
936 and more variable conditions from c. 3 cal ka, consistent with increased  
937 influence of ENSO variability during the Late Holocene.
- 938 • A distinct period of drier and / or reduced rainfall variability between 1.2 and  
939 0.9 cal ka is coincident with major hydrological changes observed across  
940 MesoAmerica. The record at Juanacatlán may reflect reduced tropical storm  
941 during a period of reduced El Niño frequency.

- 942       • A return to wetter, but more variable conditions occurred during the last c.  
943       950 years, evident from changing catchment inputs, lake stratification and  
944       nutrient availability.
- 945       • Although anthropogenic disturbance at Juanacatlán has always been  
946       relatively low, recent dramatic changes in the aquatic ecosystem highlight  
947       the sensitivity of the lake to multiple local and regional stressors.

948

949 Laguna de Juanacatlán is a key site for palaeoclimate research in Mesoamerica and  
950 provided an unambiguous record of climate over much of the last 6,000 years. The  
951 geochemical and palaeoecological record presented here provides a framework for  
952 further work to investigate ecological responses to climate change at annual or sub-  
953 annual resolution.

954

## 955 7. Acknowledgements

956

957 This paper is dedicated to the memory of Prof. Roger Byrne, who passed away  
958 shortly before this manuscript was submitted. He made numerous important  
959 contributions to Mesoamerican palaeoenvironmental research and his original work  
960 at Juanacatlán in 1990 recognised the importance of this site. We are grateful for his  
961 support and encouragement over many years.

962

963 We are very pleased to contribute to this special issue honouring the substantial  
964 contributions of Neil Roberts and Henry Lamb to palaeolimnology and to our  
965 understanding of tropical and Mediterranean palaeoclimate. We have all benefited  
966 from their insights and collaborative approach. SJD thanks Henry Lamb for his  
967 support and mentorship as an Aberystwyth University colleague which has  
968 developed into a longstanding and rewarding collaboration in research and teaching.  
969 SEM thanks Neil Roberts for many years of enjoyable discussions about the  
970 palaeoclimates of the Eastern Mediterranean and the Neotropics. Chili-Kebab lives!

971

972 We thank colleagues from the Lacustrine Core Repository, University of Minnesota,  
973 the Universidad Nacional Autonoma de Mexico (UNAM) and the Universidad

974 Michoacana de San Nicolas de Hidalgo (UMSNH), who were involved in coring as part  
975 of the MesOamerican Lakes Expedition (MOLE). Fieldwork in 2003 was supported by  
976 The University of Wales, Aberystwyth (now Aberystwyth University), the University  
977 of Nottingham, UNAM and UMSNH. Radiocarbon dating was provided through UK  
978 NERC (1108.0305) and organic geochemical analyses through the UK NERC Isotope  
979 Geosciences Facilities. BJA acknowledges receipt of a PhD studentship from the  
980 University of Wales, Aberystwyth. MC is supported by the USGS Climate and Land  
981 Use Research & Development Program. Antony Smith produced several of the  
982 figures. We appreciate constructive comments on the draft manuscript from David  
983 Wahl.

984

## 985 8. References

986

987 Almeida-Lenero, L., Hooghiemstra, H. Cleef, A.M. and van Geel, B. 2005. Holocene  
988 climatic and environmental change from pollen records of lakes Zempoala and Quila,  
989 central Mexican highlands. *Rev. Palaeobot. Palyno.* 136, 63-92.

990

991 Aston, B. J., 2008. Holocene climate variability in the Mexican Monsoon Region:  
992 stable isotope records from lake sediments. Unpubl. PhD thesis, University of Wales,  
993 Aberystwyth: 359 pp.

994

995 Battarbee R. W. 1986. Diatom Analysis. In Berglund B. E. (ed.), *Handbook of*  
996 *Holocene Palaeoecology and Palaeohydrology*. John Wiley, Chichester: 527-570.

997

998 Beekman, C. S. 2010. Recent Research in Western Mexican Archaeology. *J. Archaeol.*  
999 *Res.* 18: 41-109.

1000

1001 Bernal, J.P., Lachniet, M., McCulloch, M., Mortimer, G., Morales, P. , Cienfuegos, E.,  
1002 2011. A speleothem record of Holocene climate variability from southwestern  
1003 Mexico. *Quat. Res.* 75, 104-113.

1004

1005    Bhattacharya, T., Byrne, R., Bohnel, H., Wogau, K., Kienel, U., Ingram, B.L. and  
1006    Zimmerman, S., 2015. Cultural implications of late Holocene climate change in the  
1007    Cuenca Oriental, Mexico. *Proc. Nat. Acad. Sci.* 112, 1693-1698.  
1008  
1009    Bhattacharya T., Byrne, R., 2016. Late Holocene anthropogenic and climatic  
1010    influences on the regional vegetation of Mexico's Cuenca Oriental. *Glob. Planet.*  
1011    *Change* 138, 56-69.  
1012  
1013    Bhattacharya, T., Chiang, J. C. H., Cheng, W., 2017. Ocean-atmosphere dynamics  
1014    linked to 800 – 1050 CE drying in Mesoamerica. *Quat. Sci. Rev.* 169, 263-277.  
1015  
1016    Bonilla-Barbosa, J.R, and Novelo Retana, A. 1995. Manual de identificación de  
1017    plantas acuáticas del Parque Nacional Lagunas de Zempoala, Mexico. Cuadernos 26.  
1018    Instituto de Biología, UNAM.  
1019  
1020    Boyle, J. F., 2001. Inorganic geochemical methods in palaeolimnology. In Last WM,  
1021    Smol JP (eds) *Tracking Environmental Change Using Lake Sediments. Volume 2:*  
1022    *Physical and Geochemical Methods.* Kluwer, Dordrecht: 83-141.  
1023  
1024    Bradbury J. P. 1975. Diatom stratigraphy and human settlement in Minnesota. *Geol.*  
1025    *Soc. Am. S.P. No. 171:* 74 pp.  
1026  
1027    Bradbury, J.P., 2000. Limnologic history of Lago de Pátzcuaro, Michoacán, Mexico for  
1028    the past 48,000 years: impacts of climate and man. *Palaeogeogr. Palaeoclimatol. Palaeoecol.*  
1029    163, 69-95.  
1030  
1031    Brown. E., Johnson. T., Scholz. C., Cohen. A., King, J., 2007. Abrupt change in tropical  
1032    African climate linked to the bipolar seesaw over the past 55,000 years. *Geophys.*  
1033    *Res. Lett.* doi: 10.1029/2007GL031240  
1034  
1035

1036 Byrne, R., Allen, D., Edlund, E., Polansky, C., (1996) Can lake sediments provide a  
1037 record of tropical storms? The case of Laguna de Juanacatlán, Jalisco, Mexico  
1038 [abstract]. In: Twelfth Annual Pacific Climate (PACLIM) Workshop, 2-5 May 1995,  
1039 Asilomar Conference Center, Pacific Grove, CA, p. 159.  
1040  
1041 Caballero, M., Lozano, S., Ortega, B., Urrutia, J., Macias, J.L., 1999. Environmental  
1042 characteristics of Lake Tecocomulco, northern basin of Mexico, for the last 50,000  
1043 years. *J. Paleolimnol.* 22, 399-411.  
1044  
1045 Caballero, M., Ortega, B., Valadez, F., Metcalfe, S., Macias, J.L. , Sugiura, Y., 2002. Sta.  
1046 Cruz Atizapan: a 22-ka lake level record and climatic implications for the late  
1047 Holocene human occupation in the Upper Lerma Basin, Central Mexico.  
1048 *Palaeogeogr. Palaeoclimatol. Palaeoecol.* 186, 217-235.  
1049  
1050 Caballero, M., Vázquez, G., Lozano García, S., Rodríguez, A., Sosa Najera, S., Ruiz  
1051 Fernández, A.C. and Ortega, B. 2006: Present limnological conditions and recent (ca.  
1052 340 yr) palaeolimnology of a tropical lake in the Sierra de las Tuxtlas, eastern Mexico.  
1053 *J. Paleolimnol.* 35, 83-97.  
1054  
1055 Caballero, M., Vázquez, G., Ortega, B., Favila, M. E. and Lozano-García, S. 2016.  
1056 Responses to a warming trend and 'El Niño' in a tropical lake in western Mexico.  
1057 *Aquat. Sci* 78: 591-604.  
1058  
1059 Carmichael, I.S., Lange, R.A. and Luhr, J.F. 1996. Quaternary minettes and associated  
1060 volcanic rocks of Mascota, western Mexico: a consequence of plate extension above  
1061 a subduction modified mantle wedge. *Contrib. Miner. and Petrol.*, 124, 302-333.  
1062  
1063 Castillo, M., Muñoz-Salinas, E., Arce, J. L., Roy, P., 2017. Early Holocene to present  
1064 landscape dynamics of the tectonic lakes of west-central Mexico. *J. S.Am. Earth Sci.*  
1065 80, 120-130.  
1066

1067 Conroy, J. L., Overpeck, J. T. Cole, J. E., Shanahan, T. M., Steinitz-Kannan, M. 2008.  
1068 Holocene changes in eastern tropical Pacific climate inferred from a Galápagos lake  
1069 sediment record. *Quat. Sci. Rev.* 27: 1166-1180.

1070

1071 Correa-Metrio, A., Lozano-García, S., Xelhuantzi-Lopez, S., Sosa-Najera, S. and  
1072 Metcalfe, S.E. 2012. Vegetation in western Central Mexico during the last 50,000  
1073 years: modern analogues and climate in the Zacapu Basin. *J. Quat.Sci.* 27, 509-518.

1074

1075 Croudace, I. W., Rindby, A., Rothwell, R. G. 2006. ITRAX: description and evaluation  
1076 of a new multi-function X-ray scanner. In Rothwell, R. G. editor, *New Techniques in*  
1077 *Sediment Core Analysis*. Special Publication vol 267. Geological Society, London, 51-  
1078 63.

1079

1080 Cuna, E., Zawisza, E., Caballero, M., Ruiz-Fernandez, A.C., Lozano-García, S., Alcocer,  
1081 J., 2013. Environmental impacts of Little Ice Age cooling in central Mexico recorded  
1082 in the sediments of a tropical alpine lake. *J. Paleolimnol.* 51, 1-14, doi:  
1083 10.1007/s10933-013-9748-0.

1084

1085 Davies S. J., Metcalfe S. E., Caballero. M. E. and Juggins S. 2002. Developing diatom-  
1086 based transfer functions for Central Mexican lakes. *Hydrobiol.* 467, 199-213.

1087

1088 Davies S.J., Metcalfe S.E., MacKenzie A.B., Newton A.J., Endfield G.H., Farmer J.G.  
1089 2004 Environmental changes in the Zirahuén Basin, Michoacán, Mexico, during the  
1090 last 1000 years. *J. Paleolimnol.* 31, 77–98. doi:

1091 10.1023/B:JOPL.0000013284.21726.3d

1092

1093 Davies, S.J., Metcalfe, S.E., Bernal Brooks, F., Chacon Torres, A., Farmer, J.G.,  
1094 MacKenzie, A.B. and Newton, A.J. 2005. Lake sediments record sensitivity of two  
1095 hydrologically closed lakes in Mexico to human impact. *Ambio*, 34, 470-475.

1096

1097 Davies, S. J., Lamb, H. F., Roberts, S. J. 2015. Micro-XRF scanning applications in  
1098 palaeolimnology – recent developments. In Croudace IW and Rothwell RG (eds)

1099 Micro-XRF Studies of Sediment Cores. Developments in Palaeoenvironmental  
1100 Research series, Springer: 189-226.  
1101  
1102 Deevey, E.S., Jr. 1944. Pollen analysis and Mexican archeology, an attempt to apply  
1103 the method. *Am. Antiquity* 10, 135-149.  
1104  
1105 Denevan W. M. 1992. The pristine myth: the landscape of the Americas in 1492. *Ann.*  
1106 *Assoc. Am. Geogr.* 82, 369-385.  
1107  
1108 Douglas, M.E., Maddox, R.A., Howard, K., Reyes, S., 1993. The Mexican Monsoon. *J.*  
1109 *Clim.* 6, 1665-1776.  
1110  
1111 Douglas, P. M., Pagani, M., Canuto, M. A., Brenner, M., Hodell, D. A., Eglinton, T. E.,  
1112 Curtis, J. A., 2015. Drought, agricultural adaptation and socio-political collapse in the  
1113 Maya lowlands. *Proc. Nat. Acad. Sci.* 112, 5607-5612.  
1114  
1115 Engstrom DR, Wright, HE Jr 1984. Chemical stratigraphy of lake sediments as a  
1116 record of environmental change. In Haworth EY and Lund JWG (eds) *Lake sediments*  
1117 *and environmental history*, Leicester University Press: 11-68.  
1118  
1119 Faegri, K., Iversen, J., 1989: *Textbook of pollen analysis*. John Wiley and Sons.  
1120  
1121 Figueroa-Rangel, B.L., Willis, K.J. and Olvera-Vargas, M. 2008. 4200 years of pine-  
1122 dominated upland forest dynamics in west-central Mexico: human or natural legacy?  
1123 *Ecology* 89, 1893-1907.  
1124  
1125 Fisher, C. T., Pollard, H. P., Israde-Alcántara, I., Garduño-Monroy, V. H., Banerjee, S.  
1126 K., 2003. A re-examination of human-induced change within the Lake Pátzcuaro  
1127 Basin, Michoacán, Mexico. *Proc. Nat. Acad. Sci.* 100, 4957-4962.  
1128  
1129 Galimov E. M. 1995. *The biological fractionation of isotopes*. Academic Press, New  
1130 York, 261 pp.

1131  
1132 Gasse F. 1986. East African Diatoms. Taxonomy, ecological distribution. Bibliotheca  
1133 Diatomologica Vol. 11. J. Cramer, Stuttgart: 202 pp.  
1134  
1135 Goman, M., Joyce, A., Lund, S., Pearson, C., Guerra, W., Dale, D., Hammond, D. E.,  
1136 Celestian, A. J., 2018. Preliminary results from Laguna Minucúa a potentially annually  
1137 resolved record of climate and environmental change for the past ~5000 years in  
1138 the Mixteca Alta of Oaxaca, Mexico. Quat. Int. 469, Part B: 85-95.  
1139  
1140 Guerrero-Hernández, R., González-Gallegos, J.G. and Castro-Castro, A. 2014. Análisis  
1141 florístico de un bosque de *Abies* y el bosque mesófilo de montaña adyacente en  
1142 Juanacatlán, Mascota, Jalisco, México. Bot. Sci. 92, 541-562.  
1143  
1144 Hill, M.O. and Gauch, H.G., 1980. Detrended Correspondence Analysis: An Improved  
1145 Ordination Technique. Vegetatio 42: 47–58.  
1146  
1147 Hodell, D.A., Curtis, J.H., Brenner, M., 1995. Possible role of climate in the collapse of  
1148 Classic Maya civilization. Nature 375, 391-394.  
1149  
1150 Hodell, D.A., Brenner, M., Curtis, J.H., 2005. Terminal Classic drought in the northern  
1151 Maya lowlands inferred from multiple sediment cores in Lake Chichancanab  
1152 (Mexico). Quat. Sci. Rev. 24, 1413-1427.  
1153  
1154 IMTA, 1996. Extractor Rapido de Informacion Climatico (ERIC), CD-Rom. Instituto  
1155 Municipal de Tecnologia y Agua, Mexico.  
1156  
1157 Jones, M. D., Metcalfe, S. E., Davies, S. J. Noren, A. 2015. Late Holocene climate  
1158 reorganisation and the North American Monsoon. Quat. Sci. Rev. 124, 290-295.  
1159  
1160 Kilham, P., Kilham, S. S., Hecky, R. E. 1986. Hypothesized resource relationships  
1161 among African planktonic diatoms. Limnol. Oceanogr. 31, 1169-1181.  
1162

- 1163 Krammer K. and Lange-Bertalot H. 1986. Süßwasserflora von Mitteleuropa.  
1164 Bacillariophyceae. 1. Teil: Naviculaceae. Vol. 2/1. Gustav Fischer Verlag, Stuttgart:  
1165 876 pp.  
1166
- 1167 Krammer K. and Lange-Bertalot H. 1988. Süßwasserflora von Mitteleuropa.  
1168 Bacillariophyceae. 2. Teil: Epithemiaceae, Bacillariaceae, Surirellaceae. Vol. 2/2.  
1169 Gustav Fischer Verlag, Stuttgart: 596 pp.  
1170
- 1171 Krammer K. and Lange-Bertalot H. 1991a. Süßwasserflora von Mitteleuropa.  
1172 Bacillariophyceae. 3. Teil: Centrales; Fragilariaceae, Eunotiaceae. Vol. 2/3. Gustav  
1173 Fischer Verlag, Stuttgart: 576 pp.  
1174
- 1175 Krammer K. and Lange-Bertalot H. 1991b. Süßwasserflora von Mitteleuropa.  
1176 Bacillariophyceae. 4. Teil: Achnanthaceae. Vol. 2/4. Gustav Fischer Verlag, Stuttgart:  
1177 437 pp.  
1178
- 1179 Lachniet, M.S., Bernal, J.P., Asmerom, Y., Polyak, V. , Piperno, D., 2012. A 2400 yr  
1180 Mesoamerican rainfall reconstruction links climate and cultural change. *Geology*  
1181 doi:10.1130/G32471.1  
1182
- 1183 Lachniet, M. S., Asmerom, Y., Polyak, V., Bernal, J. P., 2017. Two millennia of  
1184 Mesoamerican monsoon variability driven by Pacific and Atlantic synergistic forcing.  
1185 *Quat. Sci. Revs.* 155, 100-113.  
1186
- 1187 Leng M.J. and Marshall J.D. 2004. Palaeoclimate interpretation of stable isotope data  
1188 from lake sediments. *Quat. Sci. Revs.*23, 811-  
1189 Leng, M.J., Metcalfe, S.E. and Davies, S.J. 2005. Investigating Late Holocene climate  
1190 variability in central Mexico using carbon isotope ratios in organic materials and  
1191 oxygen isotope ratios from diatom silica within lacustrine sediments. *J. Paleolimnol.*  
1192 34, 413-431.  
1193

1194 Lozano-García, S. 1989. Palinología y paleoambientes Pleistocénicos de la Cuenca de  
1195 Mexico. *Geofis. Int.* 28, 335-362.  
1196  
1197 Lozano-García, S., Vázquez-Selem, L., 2005. A high-elevation Holocene pollen record  
1198 from Iztaccíhuatl volcano, central Mexico. *Holocene* 15, 329-338.  
1199  
1200 Lozano García, M.S. and Xelhauntzi Lopez, M.S. 1997. Some problems in the Late  
1201 Quaternary pollen records of central Mexico: Basins of Mexico and Zacapu. *Quat.*  
1202 *Int.* 43/44, 117-123.  
1203  
1204 Lozano García, M, S. and Ortega-Guerrero, B. 1998. Late Quaternary environmental  
1205 changes of the central part of the Basin of Mexico; correlation between Texcoco and  
1206 Chalco Basins. *Rev.Palaeobot. Palyno.* 99, 77-93.  
1207  
1208 Lozano García, S., Torres-Rodriguez, E., Ortega, B., Vázquez, G. and Caballero, M.  
1209 2013. Ecosystem responses to climate and disturbances in western central Mexico  
1210 during the late Pleistocene and Holocene. *Palaeogeogr., Palaeoclimatol., Palaeoecol.*  
1211 370, 184-195.  
1212  
1213 Mackareth F.G.H.1966. Some chemical observations on post-glacial lake sediments.  
1214 *Phil. Trans. Roy.Soc. London B* 250: 165-213.  
1215  
1216 Metcalfe S. E., 1988. Modern diatom assemblages in Central Mexico: the role of  
1217 water chemistry and other factors as indicated by TWINSPAN and DECORANA.  
1218 *Freshwat. Biol.:* 217-233.  
1219  
1220 Metcalfe S. E., 1995. Holocene environmental change in the Zacapu Basin, Mexico: a  
1221 diatom based record. *Holocene* 5: 196-208.  
1222  
1223 Metcalfe, S.E., Street-Perrott, F.A., Perrott, R.A., Harkness, D.D., 1991.  
1224 *Palaeolimnology of the Upper Lerma Basin, Central Mexico.: a record of climatic*

1225 change and anthropogenic disturbance since 11,600 yr BP. *J. Paleolimnol.* 5, 197-  
1226 218.  
1227  
1228 Metcalfe S. E. Street-Perrott, F. A., O'Hara S. L., Hales P. E. and Perrott R. A. 1994.  
1229 The Palaeolimnological Record of Environmental Change: Examples from the Arid  
1230 Frontier of Mesoamerica. In: Millington A. C. and Pye K. (eds), *Environmental Change*  
1231 *in Drylands: Biogeographical and Geomorphological Perspectives*. John Wiley and  
1232 Sons Ltd, London: 131-145.  
1233  
1234 Metcalfe, S.E., O'Hara, S.L., Caballero, M. , Davies, S.J., 2000. Records of Late  
1235 Pleistocene-Holocene climatic change in Mexico – a review. *Quat. Sci. Rev.* 19, 699-  
1236 721.  
1237  
1238 Metcalfe, S., Davies, S., 2007. Deciphering recent climate change in central Mexican  
1239 lake records. *Clim. Change* 83, 169-186.  
1240  
1241 Metcalfe, S.E., Davies, S.J., Braisby, J.D., Leng, M.J., Newton, A.J., Terrett, N.L.,  
1242 O'Hara, S.L., 2007. Long and short-term change in the Patzcuaro Basin, central  
1243 Mexico. *Palaeogeogr. Palaeoclimatol. Palaeoecol.* 247, 272-295.  
1244  
1245 Metcalfe, S.E., Jones, M.D., Davies, S.J., Noren, A., MacKenzie, A., 2010. Climate  
1246 variability over the last two millennia in the North American Monsoon region  
1247 recorded in laminated sediments from the Laguna de Juanacatlán, Mexico. *Holocene*  
1248 20, 1195-1206.  
1249  
1250 Metcalfe, S.E., Barron, J.A. & Davies, S.J., 2015. The Holocene history of the North  
1251 American Monsoon: 'known knowns' and 'known unknowns' in understanding its  
1252 spatial and temporal complexity. *Quat. Sci. Rev.* 120, 1-27.  
1253  
1254 Meyers, P., 1994. Preservation of elemental and isotopic source identification of  
1255 sedimentary organic matter. *Chem. Geol.* 114, 289-302.  
1256

1257 Meyers, P. A., Lallier-Verges, E., 1999. Lacustrine sedimentary organic matter records  
1258 of Late Quaternary paleoclimates. *J. Paleolimnol.* 21: 345-372  
1259

1260 Meyers P.A. and Teranes J.L. 2001. Sediment Organic Matter. Last, W.M. and Smol,  
1261 J.P. (eds). *Tracking Environmental Change Using Lake Sediments. Vol 2: Physical and*  
1262 *Geochemical Methods.* Kluwer Academic Publishers, Dordrecht, The Netherlands.  
1263

1264 Mountjoy, J. B., 2012. *Arte Rupestre en Jalisco.* Conaculta, Gobierno Federal, y  
1265 Secretaría de Cultura, Gobierno de Jalisco. Acento Editores. Guadalajara, Jalisco.  
1266 México: 46 pp.  
1267

1268 O'Hara S. L., Street-Perrott F. A. and Burt T. P. 1993. Accelerated soil erosion around  
1269 a Mexican highland lake caused by Pre-Hispanic Agriculture. *Nature* 362: 48-51.  
1270

1271

1272 Ortega, B., Vázquez, G., Caballero, M., Israde, I., Lozano-García, S., Schaaf, P., Torres,  
1273 E., 2010. Late Pleistocene: Holocene record of environmental changes in Lake  
1274 Zirahuén, Central Mexico. *J. Paleolimnol.* 44, 745-760, doi:10.1007/s10933-010-  
1275 9449-x.  
1276

1277 Ortega Rosas, C.I., Peñalba, M.C. and Guiot, J. 2008 Holocene altitudinal shifts in  
1278 vegetation belts and Environmental changes in the Sierra Madre Occidental,  
1279 northwestern Mexico, based on modern and fossil pollen data. *Rev. Palaeobot,*  
1280 *Palynol.* 151, 1-20.  
1281

1282 Ownby, S., Lange, R., Hall, C., 2008. The eruptive history of the Mascota volcanic  
1283 field, western Mexico: Age and volume constraints on the origin of andesite among a  
1284 diverse suite of lamprophyric and calc-alkaline lavas. *J. Volcanol. Geoth. Res.* 177,  
1285 1077-1091.  
1286

1287 Palacios-Chavez, R., (1968). *Morfología de los granos de polen de árboles del Estado*  
1288 *de Morelos.* *Anales de la Escuela Nacional de Ciencias Biológicas* 16, 41-169.

1289

1290 Palacios-Chavez, R., (1985). Lluvia de polen moderno en el bosque tropical  
1291 caducifolio de la estación de Biología de Chamela, Jal., (México). Anales de la Escuela  
1292 Nacional de Ciencias Biológicas 29, 43-55.

1293

1294 Park, J., Byrne, R., Bohnel, H., Molina Garz, R and Conserva, M. 2010. Holocene  
1295 climate change and human impact, central Mexico: a record based on maar lake  
1296 pollen and sediment chemistry. Quat. Sci. Rev. 29, 618-632.

1297

1298 Ramos Zamora, D. 1977. Morfología de los granos de polen de la familia Moraceae  
1299 en Mexico. B. Soc. Bot. Méx. 36, 71-92.

1300

1301 Reimer, P., Baillie., M. G, Bard, E., Bayliss, A., Beck, J., Bertrand, C., et al., 2004.  
1302 IntCal04 terrestrial radiocarbon age calibration, 0–26 cal kyr BP. Radiocarbon 46,  
1303 1029–1058.

1304

1305 Rhodes, J. A., Mountjoy, J. B., Cupul-Magaña, F. B., 2016. Understanding the  
1306 wrapped bundle burials of west Mexico: a contextual analysis of Middle Formative  
1307 mortuary practices. Ancient Mesoam. 27, 377-388.

1308

1309 Rodríguez-Ramírez, A., Caballero, M., Roy, P., Ortega, B., Vázquez-Castro, G., Lozano-  
1310 García, S., 2015. Climatic variability and human impact during the last 2000 years in  
1311 western Mesoamerica: evidence of late Classic (AD 600–900) and Little Ice Age  
1312 drought events. Climate of the Past 11, 1239-1248

1313

1314 Rodysill, J. R., Anderson, L., Cronin, T. M., Jones, M. C., Thompson, R. S., Wahl, D. B.,  
1315 Willard, D. A., Addison, J. A., Alder, J. R., Anderson, K. H., Anderson, L., Barron, J. A.,  
1316 Bernhardt, C. E., Hostetler, S. W., Kehrwald, N., M., Khan, N. S., Richey, J. N., Starratt,  
1317 S. W., Strickland, L. E., Toomey, M. R., Treat, C., Wingard, L. E., 2018. A North  
1318 American Hydroclimate Synthesis (NAHS) of the Common Era. Glob. Planet.Change  
1319 162: 175-198.

1320

1321 Ropelewski, C.F., Gutzler, D.S., Higgins, R.W. , Mechoso, C.R., 2005. The North  
1322 American Monsoon System, in: Change, C-P, Wang, B. and Lau, N.C.G. (Eds.), The  
1323 Global Monsoon System: Research and forecast. WMO Technical Document 1266,  
1324 Geneva, pp. 207-218.  
1325  
1326 Rühland, K. M., Paterson, A. M., Smol, J. P., 2015. Lake diatom responses to  
1327 warming: reviewing the evidence. J. Paleolimnol. 54: 1-35.  
1328 Rzedowski, J. 1994. Vegetación de México. Limusa, Mexico. 432pp.  
1329  
1330 Saros, J. E., Michel, T. J., Interlandi, S. J., Wolfe, A. P., 2005. Resource requirements  
1331 of *Asterionella formosa* and *Fragilaria crotonensis* in oligotrophic alpine lakes:  
1332 implications for recent phytoplankton community reorganizations. Can. J. Fish.  
1333 Aquat. Sci. 62: 1681–1689.  
1334  
1335 Saros, J. E., Clow, D. W., Blett, T., Wolfe, A.P., 2011. Critical nitrogen deposition loads  
1336 in high-elevation lakes of the western US inferred from paleolimnological records.  
1337 Wat. Air Soil Poll. 216: 193–202.  
1338  
1339 Saros, J. E., Stone, J. R., Pederson, G. T., Slemmons, K. E. H., Spanbauer, T., Schliep.  
1340 A., Cahl, D., Williamson, C. E., Engstrom, D. R., 2012. Climate-induced changes in lake  
1341 ecosystem structure inferred from coupled neo-and paleoecological approaches.  
1342 Ecology 93: 2155–2164.  
1343  
1344 Schnurrenberger, D., Russell, J., Kelts, K. 2003: Classification of lacustrine sediments  
1345 based on sedimentary components. J. Paleolimnol. 29, 141-154.  
1346  
1347 Sears, P.B. 1952. Palynology in southern North America. I: Archeological horizons in  
1348 the basins of Mexico. Bull. Geol. Soc. Am. 63, 241-254.  
1349  
1350 Serrato, A., Ibarra-Manriquez, G. and Oyama, K. 2004. Biogeography and  
1351 conservation of the genus *Ficus* (Moraceae) in Mexico. J. Biogeogr. 31, 475-485.  
1352

1353 Sigala, I., Caballero, M., Correa-Metrio, A., Lozano-García, S., Vázquez, G., Pérez, L.,  
1354 Zawisza, E., 2017. Basic limnology of 30 continental waterbodies of the Transmexican  
1355 Volcanic Belt across climatic and environmental gradients. *Bol. Soc. Geol. Mex.* 69,  
1356 313-370.  
1357  
1358 Sosa-Najera, S., Lozano-García, S., Roy, P.D., Caballero, M., 2010. Registro de sequías  
1359 históricas en el occidente de México con base en el análisis elemental de sedimentos  
1360 lacustres: el caso del lago de Santa María del Oro. *Bol. Soc. Geol. Mex.* 62, 437-451.  
1361  
1362 Stahle, D.W., Burnette, D.J., Villanueva Diaz, J., Heim, R.R., Jr., Fye, F.K., Cerano  
1363 Paredes, J. Acuna Soto, R., Cleaveland, M.K., 2012a. Pacific and Atlantic influences on  
1364 Mesoamerica climate over the past millennium. *Clim. Dynam.* 39, 1431-1446,  
1365 doi:10.1007/s00382-011-1205-z.  
1366  
1367 Vázquez-Castro, G., Ortega, B., Davies, S.J., Aston, B.J., 2010. Registro sedimentario  
1368 de los últimos ca. 17000 años del lago de Zirahuén, Michoacán, Mexico. *Bol. Soc.*  
1369 *Geol. Mex.* 62, 325-343.  
1370  
1371 Vázquez-Castro, G., Ortega-Guerrero, B., Rodríguez, A., Caballero, M., Lozano-García,  
1372 S., 2008. Mineralogía magnética como indicador de sequía en los sedimentos  
1373 lacustres de los últimos ca. 2600 años de Santa Maria del Oro. *Rev. Mex. Cienc.*  
1374 *Geol.* 25, 21-38.  
1375  
1376 Watts, W.A. and Bradbury, J.P. 1982. Paleoecological studies at Lake Patzcuaro on  
1377 the west-central Mexican plateau and at Chalco in the Basin of Mexico. *Quat.Res.*  
1378 17, 65-70.  
1379  
1380 Woodbridge, J., Roberts, N., 2011. Late Holocene climate of the Eastern  
1381 Mediterranean inferred from diatom analysis of annually-laminated lake sediments.  
1382 *Quat. Sci. Rev.* 30, 3381-3392.  
1383

1384 Yang, J.R., Pick, F.R., Hamilton, P.B., 1996. Changes in the planktonic diatom flora of  
1385 large mountain lake in response to fertilization. *J. Phycol.* 32: 232–243.  
1386